ORGANIC MATTER AND NON-REFRACTORY AEROSOL OVER THE REMOTE SOUTHEAST PACIFIC OCEAN: OCEANIC AND COMBUSTION SOURCES

A THESIS SUBMITTED TO THE GRADUATE DIVISION OF THE UNIVERSITY OF HAWAIʻI IN PARTIAL FULFILLMENT OF THE REQUIREMENTS FOR THE DEGREE OF

MASTER OF SCIENCE

IN

OCEANOGRAPHY

DECEMBER 2011

By
Lindsey Shank

Thesis Committee:

Antony Clarke, Chairperson
Steven Howell
Barry Huebert

TABLE OF CONTENTS

LIST OF TABLES

LIST OF FIGURES

1 Introduction

1.1 Aerosol

The Earth's atmosphere contains significant concentrations of tiny suspended particles called aerosol. Depending on location, aerosol concentrations can range from ~10 - 100 per cm^{-3} in the polar regions (Bodhaine et al., 1986), to a couple hundred particles per cm^{-3} of air in the remote marine atmosphere, to 10^7-10^8 cm^{-3} in urban environments (Seinfeld and Pandis, 2006). Aerosol can have several important effects, including impacts on human health, visibility, and Earth climatic effects (Jacob, 1999).

1.1.1 Aerosol size distributions, generation, and removal processes

Particle size is largely dependent on the generation mechanism and source of the aerosol, as well as loss mechanisms (Jacob, 1999). Aerosols can be loosely grouped into three general categories based on particle size. Depending on location and conditions, the size cut-offs are defined differently. The smallest group are particles (generally < 0.1 μm in diameter (d_a)), which arise from gas to particle conversion of vapors emitted from various sources, such as the surface of the ocean or from combustion. These particles are short-lived, as they have a high diffusivity and tend to coagulate to form larger particles (fine particles, ranging from ~ $0.1 < d_a < 1$ μm). Fine particles make up the accumulation mode of the aerosol size distribution (see Fig. 1), as they are too big to coagulate and grow through condensation, but are more resistant to gravitational settling than larger particles. Therefore, in the absence of wet deposition (i.e., precipitation), there are no effective removal mechanisms for these particles, thus they accumulate in the atmosphere. Coarse particles are generally defined as particles with $d_a > 1$ μm. Coarse particles tend to be mechanically generated, such as from the wind acting on the surface of the earth to

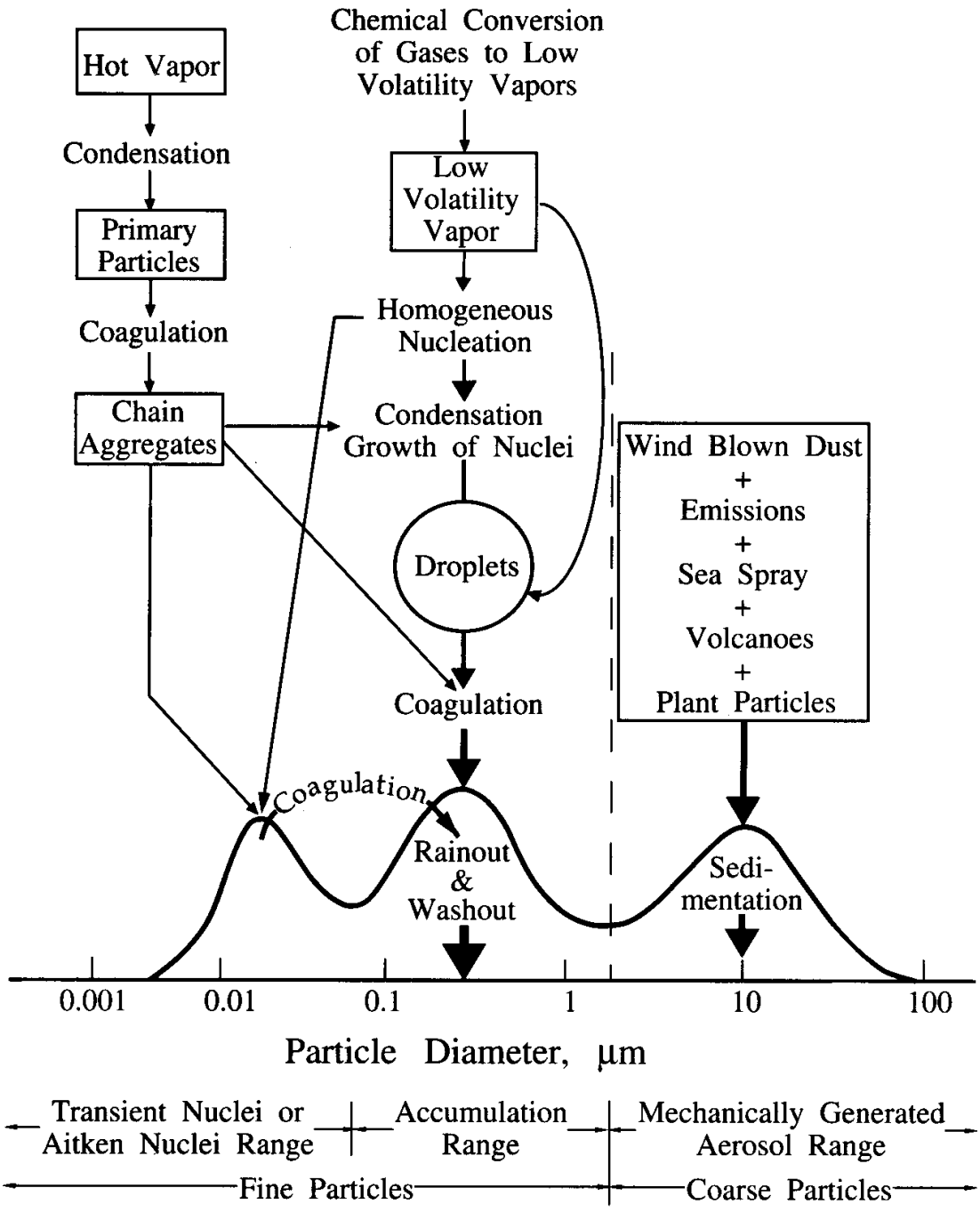

Figure 1. The three general modes of particles, and their sources and removal mechanisms. Adapted from Seinfeld and Pandis, 2006.

produce sea-spray and dust. Figure 1 is a schematic of an idealized size distribution showing the three modes along with the generation and sources of the different sizes of

aerosol, as well as several removal mechanisms for each mode. While smaller particles are often lost to coagulation, coarse particles are lost to gravitational settling, and accumulation mode particles to precipitation (wet deposition) (Jacob, 1999; Seinfeld and Pandis, 2006). While these general groupings hold true overall, any given distribution can vary in the relative magnitude and mean diameters of the modes. These reflect size-dependent variations in source strengths, atmospheric processes, lifetimes and removal mechanisms.

1.1.2 Aerosol chemistry

Atmospheric particles are composed of sulfates (SO_4), nitrates (NO_3), ammonium (NH_4), organic material (OM), crustal material, sea-salt, trace metals usually in the form of oxides, and water (Seinfeld and Pandis, 2006). Sulfuric acid (H_2SO_4) is a typical precursor gas, produced in the atmosphere through oxidation of sulfur dioxide (SO_2), emitted from sources such as fossil fuel combustion, smelters, and volcanoes (Jacob, 1999). Once in the atmosphere, SO_2 can be oxidized to SO_4. SO_4 contributes largely to total fine aerosol mass in typical tropospheric aerosols. NH_4, OM, elemental carbon (EC) (i.e., soot or black carbon (BC)), and some transition metals are also found predominately in the fine mode. Trace elements are introduced from sources such as combustion of coal, oil, wood burning, steel furnaces, boilers, smelters, dust, waste incineration, and brake wear (Seinfeld and Pandis, 2006). Their size depends on their origin. Crustal species include silicon, calcium, magnesium, aluminum, and iron. These, along with trace metals, and some OM (i.e., plant fragments from processes such as biomass burning) are often associated with coarse particles. Sea-salt is also a major component of coarse particle composition, and dominates the coarse mass in the remote marine atmosphere.

NO_3 is found on both coarse and fine particles. On fine particles it is often found as ammonium nitrate (NH_4NO_3), while on coarse particles it is the result of nitric acid (HNO_3) reactions with sodium chloride (NaCl or sea-salt) or crustal material (dust) (Seinfeld and Pandis, 2006).

Table 1 summarizes the formation pathways, chemical composition, sources, and atmospheric lifetimes of the three particle modes.

Table 1. Comparison of Ambient and Fine and Coarse Particles

	Fine Particles	Coarse Particles
Formation pathways	Chemical reactions	Mechanical disruption
	Nucleation	Suspension of dusts
	Condensation	
	Coagulation	
	Cloud/fog processing	
Composition	Sulfate	Resuspended dust
	Nitrate	Coal and oil fly ash
	Ammonium	Crustal elements (Si, Al, Ti, Fe)
	Hydrogen ion	oxides
	Elemental carbon	$CaCO_3$, NaCl
	Organic compounds	Pollen, mold, spores
	Water	Plant, animal debris
	Metals (Pb, Cd, V, Ni, Cu, Zn, Mn, Fe, etc)	Tire wear debris
Solubility	Largely soluble, hydroscopic	Largely insoluble and non-hydroscopic
Sources	Combustion (coal, oil, gasoline, diesel, wood)	Resuspension of industrial dust and soil
	Gas-to-particle conversion of NO_x, SO_3, and VOCs)	Suspension of soil (farming, mining, unpaved roads)
	Smelters, mills, etc.	Biological sources
		Construction/demolition
		Ocean spray
Atmospheric lifetime	Days to weeks	Minutes to days
Travel distance	100s to 1000s of km	< to 10s of km

Coarse and fine size categories refer to mean particle diameter above and below 2.5 μm, respectively

Source: Seinfeld and Pandis (2006)

1.2 Aerosol and climate

Humans perturb the atmosphere through the emissions of not only climate-forcing greenhouse gases, but particulate matter as well. Industrial processes, fossil fuel combustion, and food-cooking are examples of anthropogenic activities that can influence not only local air quality, but can have regional and even global impacts.

Aerosol can affect global climate in two basic ways commonly referred to as the aerosol "direct effect" and the "indirect effect". Aerosol directly scatters and absorbs incoming solar radiation in ways that can contribute to changes in the global radiation balance. Forcing, as it relates to climate science, is defined as the change in net irradiance (in units of W m^{-2}) at the top of the atmosphere. The magnitude of the effect characterized as "direct forcing" is a measure of changes in the amount of radiation scattered back to space (Seinfeld and Pandis, 2006) due directly to changes in atmospheric aerosol.

The "indirect effect" refers to the impact on radiation caused by changes in cloud properties. This is because aerosol particles act as a cloud condensation nuclei (CCN), a "seed" for the condensation of water vapor from which a cloud can form. There are many hypothesized cloud effects, the first attributed to Twomey (1977), who suggested that increased concentrations of atmospheric aerosol will result in higher concentrations of CCN, leading to a larger amount of smaller cloud droplets. Albrecht (1989) suggested that because droplets are smaller a larger liquid water path is maintained, which suppresses precipitation and results in more reflective clouds. Both "indirect effects" lead to higher cloud albedos. The "indirect effect" is observed to be strongest in clouds with a relatively small number of droplets (i.e., remote marine stratocumulus decks)

(Baker and Charlson, 1990). Figure 2 illustrates some of the effects (both the "direct effect" and numerous "indirect effects", such as those described above). Properties of the aerosol such as size, abundance, and chemistry determine how effectively it will scatter incoming solar radiation back to space, and these properties also influence how effective a CCN a particle will be.

The International Panel on Climate Change (IPCC) identifies sources of climate forcing, and the associated magnitude and sign of that forcing. Figure 3 (IPCC, 2007) shows some of the different sources of radiative forcing that have been identified, and the estimates of the magnitude and sign of each source. Although the signs of both aerosol effects are negative (i.e., cooling effect), the magnitude of the radiative forcing remains uncertain, particularly for the "indirect effect", as shown by the large error bars on the aerosol effects in Fig. 3 (here referred to as the cloud albedo effect).

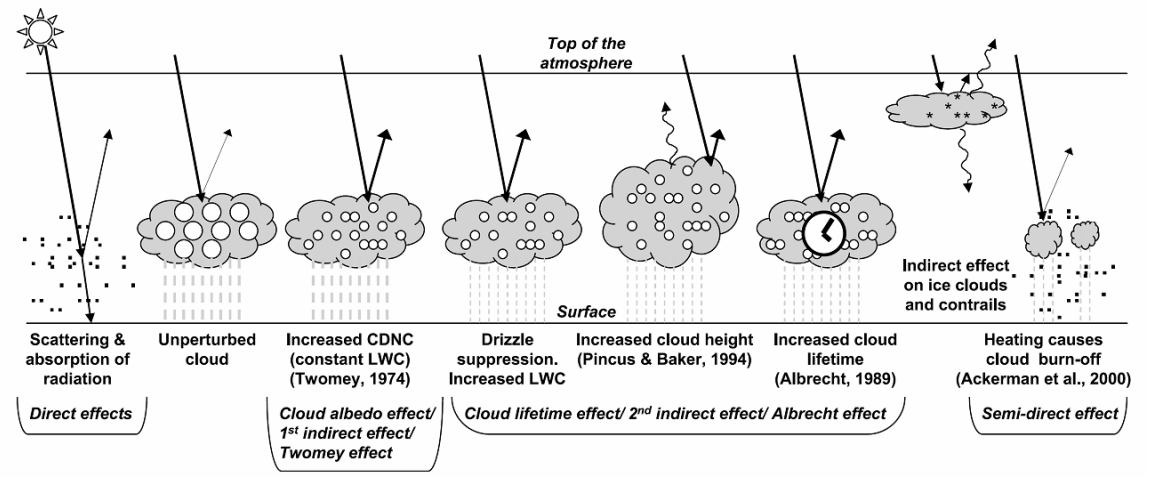

Figure 2. Direct effect of aerosol on scattering and absorption of incoming solar radiation, as well as illustrations of the many cloud indirect effects. CDNC= Cloud droplet number concentration, LWC=liquid water content. Source: IPCC, 2007.

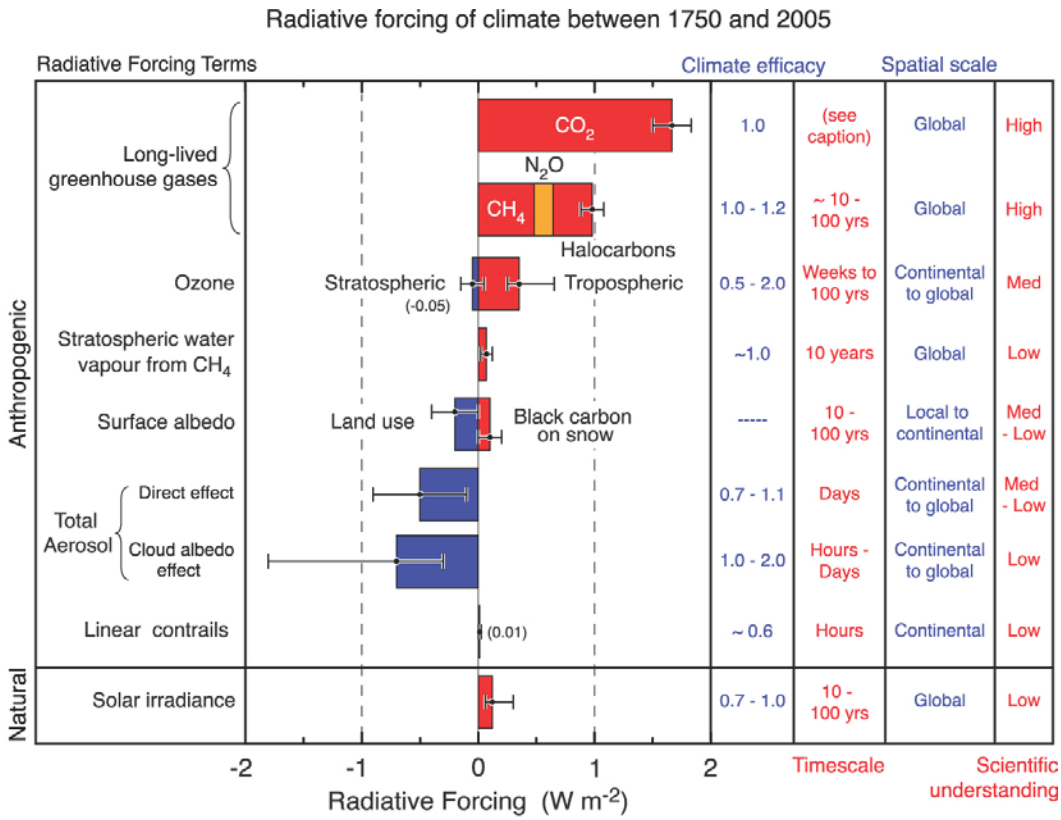

Figure 3 IPCC sources of radiative forcing and the estimated magnitude and sign. The sources are listed based on their level of scientific understanding (far right column). Source: IPCC, 2007.

Forcing terms are also listed based on their level of scientific understanding. Note that the direct and indirect effect are listed at the medium-low and low level, respectively. The latter two observations suggest that more research in the areas of aerosol climatic effects is required.

1.3 Marine aerosol

In the marine boundary layer (MBL) over the remote ocean and far removed from anthropogenic influences, the ocean surface is a major source of aerosol mass and number. Wind blowing on the surface of the ocean produces sea-spray aerosol and facilitates bubble-bursting, which produces a primary marine aerosol made up of a

combination of sea-salt and OM (Jacob, 1999). It is estimated that sea-salt production is around 1-3 × 10^{16} g yr^{-1} (O'Dowd and DeLeeuw, 2007). Gas to particle conversion of vapors emitted to the atmosphere from oceanic phytoplankton (i.e., dimethylsulfide (DMS)) (Andreae and Raemdonck, 1983; Grenfell et al., 1999) constitutes another major source of marine aerosol, termed secondary aerosol. Another source of aerosols to the remote MBL is entrainment from the free troposphere (FT) (Clarke et al., 1998). Hence, long range transport of pollution, as well as marine sources of aerosol, can increase aerosol and CCN concentrations in remote areas, thus potentially affecting the local albedo and cloud properties (Clarke et al., 2001; Clarke and Kapustin, 2010; Jaffe et al., 1999).

The roles of sea-salt aerosol and non-sea-salt sulfates in climate processes (Charlson et al., 1987; Shaw, 1983) have long motivated investigations of marine aerosol. Sulfuric acid, ammonium bisulfate, ammonium sulfate and methanesulfonate are the main aerosol from the primary organic vapor (DMS) emitted from the ocean (Charlson et al., 1987). More recently the role of organic matter (OM) in marine aerosol has been under investigation due to (at least) three things: 1) the detection of short-lived organic gases (e.g. isoprene and glyoxal) suggesting that non-DMS organic vapors may be important (Volkamer et al., 2010); 2) measurements of new particle growth rates that cannot be explained by sulfates alone (e.g. Weber et al., 1998); and 3) large quantities of OM in marine air masses (at high latitudes). Significant concentrations of organic aerosol (OA) have been observed at sites believed to represent clean marine conditions (Hoffman and Duce, 1976; Kleefeld et al., 2002; Middlebrook et al., 1998; Novakov et al., 1997; Putaud et al., 2000), making the quantification of the oceanic OA contribution to

marine aerosol a current focus of investigation. OA is formed though the oxidation, condensation, and oligomerization of various organic molecules, including hydrocarbons, alcohols, aldehydes, and carboxylic acids. Therefore, due to its complex chemical nature it has been difficult to identify, let alone quantify, the individual components of OA. This has lead to a loosely defined, broad grouping under the general term "organic matter" (Andreae, 2009).

Variables such as the degree of oxidation, molecular weight, light absorption, and hydroscopicity also determine how OA behaves in the atmosphere and how it affects climate (Andreae, 2009). Understanding and quantifying OA sources is the first step in understanding how it is distributed, and how it affects both regional and global climate. Measurements at Mace Head, Ireland, a coastal sampling site in the North Atlantic, suggest relatively large amounts of OA (up to 72 % of total aerosol mass) are linked to increased biological production (O'Dowd et al., 2004; Spracklen et al., 2008), suggesting that biogenic emissions are an important source of mostly water-insoluble, and some water soluble, OM to the remote MBL. Their results indicate the ocean is a significant source of primary OM to the remote marine atmosphere.

1.4 Motivation

To quantify how human perturbations are altering aerosol concentrations, and ultimately how increased aerosol loadings affect global climate, it is essential to determine the physical and chemical properties of aerosols which constitute a clean, or unperturbed, atmosphere. Many studies have attempted to describe a "clean" atmosphere by establishing background conditions through marine aerosol measurements from land sites and ships (Allen et al., 2004; Andreae et al., 1999; Lohmann et al., 2005; Phinney et

al., 2006; Quinn and Bates, 2003; Yoon et al., 2007). For example, Allan et al. (2004) took submicron aerosol measurements in the North Pacific from Trinidad Head, California. They used an Aerodyne Aerosol Mass Spectrometer (AMS) to take measurements of SO_4, NH_4, NO_3, and OA. They used a combination of Air Mass Back Trajectories (AMBTs), correlation with Volatile Organic Carbon species (VOCs), and an increase in OA accumulation mode mean diameter, to determine clean versus continentally influenced air masses. Phinney et al. (2006) took measurements of sea-salt, non-sea-salt SO_4 (nss-SO_4), and OA in the North Pacific (Ocean Station Papa at 50°N, 145°W), using MOUDI impactors that collected aerosols between 0.03 and 18 μm. They also used AMBTs to identify clean air cases. Another common method for determining clean conditions is using particle number concentration below a particular threshold (Cavalli et al., 2004).

Much of the work on marine OM has been at mid-to high-latitude near biologically productive regions of the ocean. Satellite-derived mean chlorophyll-*a* concentrations have been weakly correlated ($R^2 \sim 0.25$) with OC concentrations in clean marine aerosols collected over the North Atlantic (O'Dowd et al., 2004). In other studies, correlations between trajectory weighted chlorophyll-*a* and OC were also found for aerosols collected at Amsterdam Island ($R^2 = 0.60$), Mace Head ($R^2 = 0.75$), however no relationship between chlorophyll-*a* and OA was found for clean marine aerosols collected at the Azores (Spracklen et al., 2008). Zorn et al. (2008) found up to 51% of submicron non-refractory mass attributed to OA during a phytoplankton bloom in the South Atlantic but noted trajectories were recently over land.

These studies used a combination of parameters including AMBTs, wind direction, carbon monoxide (CO), and black carbon (BC) mass as criteria for establishing clean air cases. AMBTs indicating that air masses had spent at least four days advecting over the North Atlantic Ocean prior to sampling was the primary criterion for determining clean marine cases during the study conducted at Mace Head (O'Dowd et al., 2004; Spracklen et al., 2008; Yoon et al., 2007). However, unless aerosol from sources upwind have been effectively removed through precipitation, these air masses remain subject to influences from long range transport. Coastal sites can be subject to influence by higher levels of OA due to increased local ocean production, as well as terrestrial sources (Spracklen et al., 2008). Mean CO in the Mace Head air masses was 130 ± 5 ppbv, a value taken as representative of background conditions in the remote Arctic and North Atlantic environment (Cavalli et al., 2004). Like CO, BC is derived from combustion, and therefore has primarily anthropogenic and biomass burning sources. BC concentrations for Mace Head "clean" cases averaged 40 ng m^{-3}, described as background concentrations for Northern Hemisphere air masses (Cavalli et al., 2004).

BC is a product of incomplete combustion and is an unambiguous indicator of non-marine aerosol; whenever BC aerosol is found in a marine air mass it must be accompanied by other aerosol products of combustion. There are three obvious ways to handle the presence of continental influence in order to define background marine conditions: 1) try to subtract out the non-marine aerosol; 2) develop a tracer that directly indicates the marine contribution; or 3) develop thresholds which, when met, assume non-marine aerosol is negligible (the methodology used in the studies described above). The first is difficult, as it requires a tracer quantitively linked to continental OM. BC

itself is an obvious choice, but reported OM:BC ratios near source regions range widely: 20:1 and 34:1 for southwesterly and northwesterly flow from the northeast coast of the United States (Bates et al., 2005), 85:1 for fresh and 25:1 for aged Canadian forest fires (Singh et al., 2010), 1:1 from southwest India and 8:1 from northeast Asia (Quinn and Bates, 2005; INDOEX and ACE-Asia:polluted, respectively), and 8:1 from southern Africa (Haywood et al., 2003). Reid et al., (2005) show OC:BC ranging from 2 to 17 for a wide range of biomass burning, though they cluster around 11. Carbon isotopes have been used as tracers of marine organics (option 2), allowing a few groups to calculate marine and continental contributions to OM. Turekian et al., (2003), Narukawa et al. (2008), and Miyazaki et al. (2010) used ^{13}C and Ceburnis et al. (2011) used ^{14}C as well.

Even at high latitude sites, air from the subtropics tends to have much lower organic content. At Mace Head, Dall'Osto et al. (2010) found that winds from the south had $Org/SO_4 \approx 0.17$. At Amsterdam Island, Sciare et al. (2009) found low OM during Austral winter, and when back trajectories were from the north. Both of these studies found BC (45 and 7 ng m^{-3}) and neither attempted to isolate the purely marine contributions, which must have been lower. Zorn et al. (2008), reported Org/SO_4 ratios of 0.07 and 0.17 for the Antarctic and South Atlantic oceans, but had no BC or CO data. Of the carbon isotope tracer studies mentioned above, only Miyazaki et al. (2010) documented air masses from subtropical regions during non-bloom periods. They found that only 8-36% of the OM was due to marine sources during samples with back trajectories that originated over the oligotrophic central North Pacific before crossing narrow high-productivity areas to reach the ship they were sampling from. It's not clear how much of the aerosol was contributed by the low-productivity region. EC during the

Miyazaki et al. (2010) study averaged 43 ng m^{-3}. Less directly, hygroscopic growth experiments in the Southern Atlantic and Indian Oceans (Maßling 2003), the Pacific and Southern Oceans (Berg et al., 1998), near Puerto Rico (Allan et al., 2008) and the Eastern Atlantic (Allan et al., 2009) all found hygroscopic growth of aerosol particles consistent with particles composed chiefly of sulfate salts rather than OM during clean marine periods.

Studies of OA over the equatorial and southern oceans remain underrepresented relative to high and mid-latitudes. This constitutes a large gap in the understanding of OA production in marine systems. Here we present results from the Southeast and Central Pacific Ocean, areas where few aerosol measurements have been taken, in order to facilitate the understanding of global background aerosol. Results from three such experiments are discussed in this thesis and results are compared and contrasted to those from previous clean air investigations.

1.5 Experiments

1.5.1 VOCALS-REx

The Variability of the American Monsoon Systems (VAMOS) Ocean-Cloud-Land-Study Regional Experiment (VOCALS-REx), took place in October/November 2008 out of Arica, Chile. The purpose of VOCALS was to study the Southeast Pacific (SEP) climate system, more specifically how the South American continent, the SEP Ocean, and the atmosphere interact, and the coupling between them. A coastal jet results from interrupted zonal flow along the western coast of the South American continent, due to the presence of the Andes Mountain range. These strong winds run parallel to the coast of Chile and Peru, driving coastal oceanic upwelling in this area. During this

upwelling, cold, nutrient-rich waters are brought to the surface, producing sea-surface temperatures (SSTs) that are lower than SSTs at comparable latitudes elsewhere. Marine stratocumulus clouds are formed when warm, dry air aloft couples with the cold ocean surface. The largest and most persistent stratocumulus cloud deck in the world is found over the SEP, which has a major impact on Earth's radiation budget (through the reflectance of solar radiation). Understanding the factors that contribute to the persistence of this stratocumulus deck is essential in understanding how this coupled land and ocean climate system affects local and global albedo (Wood et al., 2011). Figure 4 illustrates the SEP climate system and the key features explored during VOCALS.

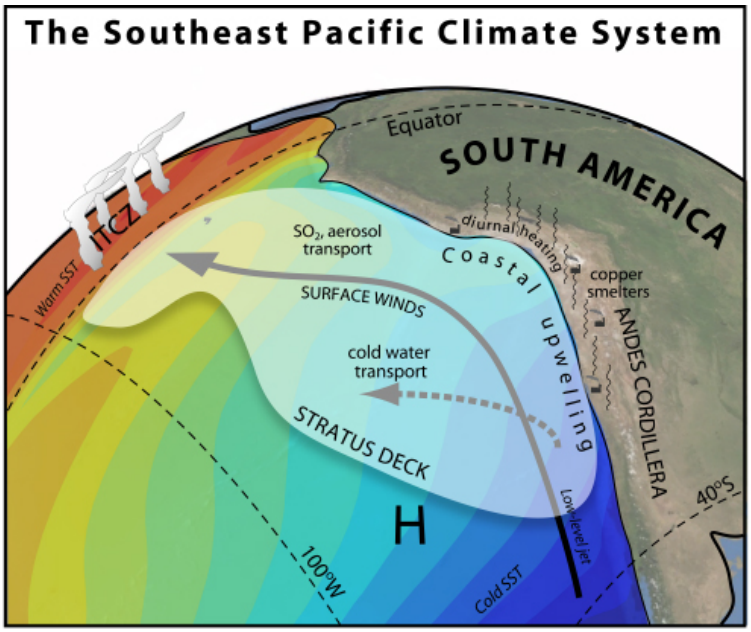

Figure 4. VOCALS-REx study area and illustration of the coupled ocean-cloud-atmosphere-land climate system. Source: Wood et al., 2011b.

Anthropogenic aerosol sources in this region include urban pollution from South American cities such as Santiago, which lies south of the VOCALS study region. Copper

smelters are also found along the western coast of Chile. The ocean surface is likely the largest contributor to natural aerosol mass. It has been hypothesized that anthropogenic aerosol is more important than natural aerosol in terms of influences on precipitation in marine stratocumulus clouds in this region, and that pollution aloft is an important source of CCN in the SEP (Wood et al., 2011b).

The campaign involved 14 research flights aboard the National Center for Aerosol Research (NCAR) C-130, with three distinct flight patterns (Wood et al., 2011b). These included 1) flights along 20°S with 10 minute legs above-cloud, in-cloud and below cloud, 2) flights investigating pockets of open cells (POCs) in the stratocumulus deck (Wood et al., 2010a), and 3) southern pollution surveys to 30°S along the coast of Chile. Figure 5 illustrates the spatial orientation of each type of flight, while Figs. 6 and 7

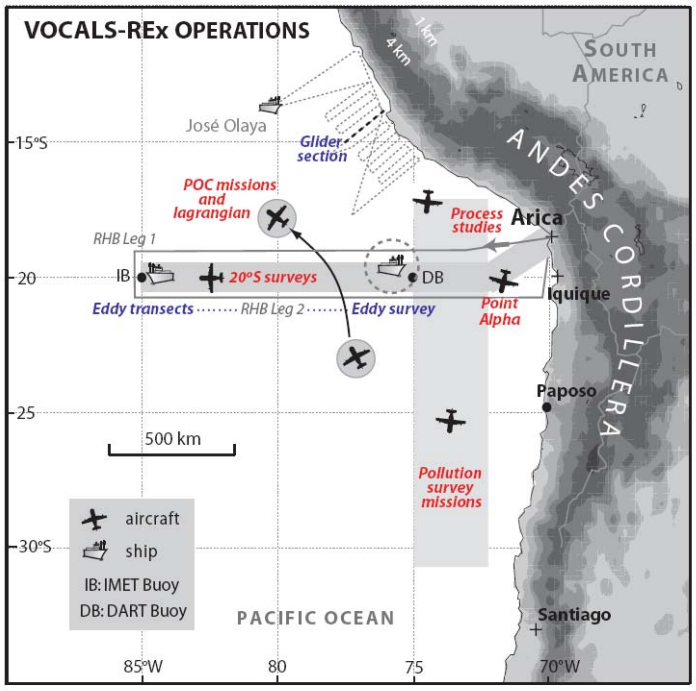

Figure 5. VOCALS field operations including illustrations of areas sampled during each type of flight, and areas covered by different research platforms. Source: Wood et al. (2011b).

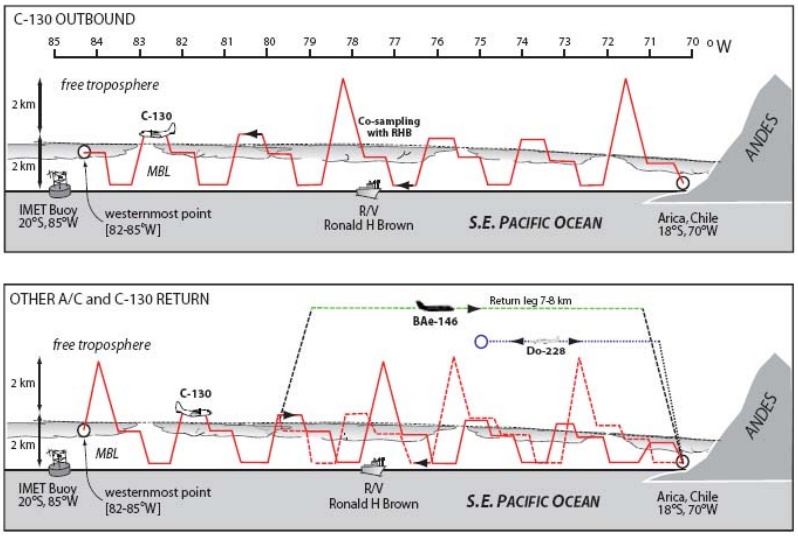

Figure 6. Cross section of a stacked-leg flight pattern for the NCAR C-130. Source: Wood et al. (2011b)

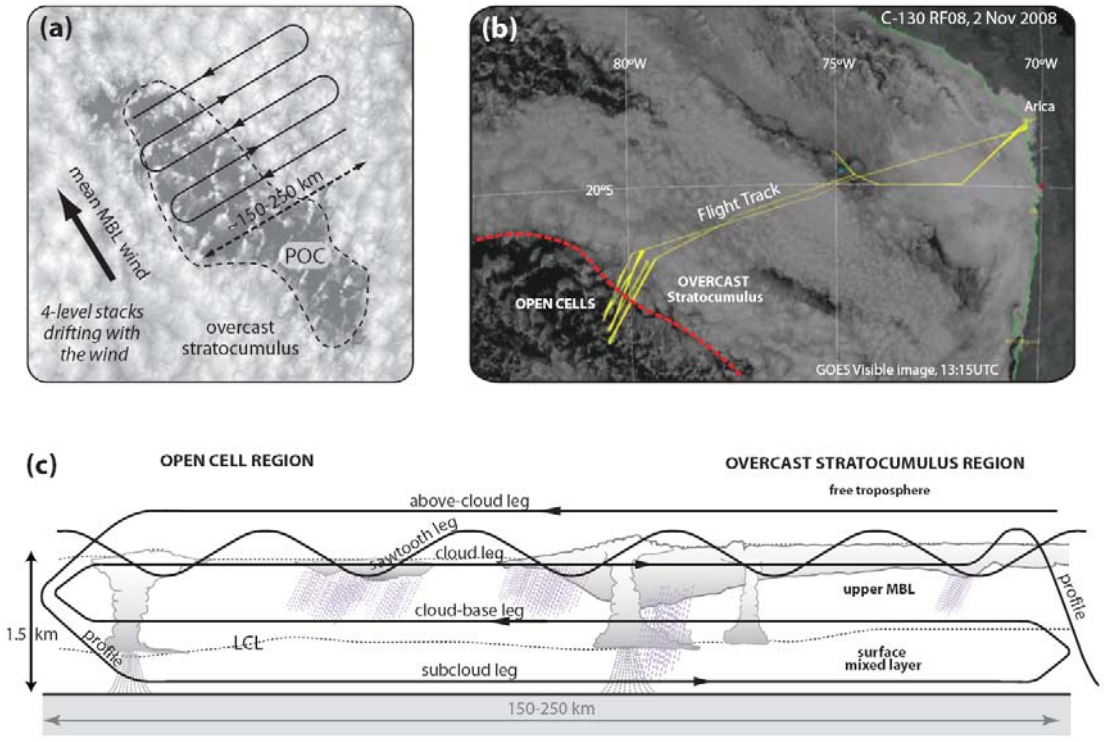

Figure 7. POC mission **(a)** schematic of flight and illustration of POC; **(b)** example POC mission flight track from C-130 Research Flight RF08 on 2 Nov 2008; **(c)** cross section of flight. Source: Wood et al. (2011b).

illustrate the different types of flight patterns. Figure 6 shows a typical cross section of a 20°S survey with stacked legs, and Fig. 7 illustrates the flight pattern and schematic for a POC mission. For an entire synopsis of the VOCALS operations see Wood et al. (2011b). Other aircraft involved in the campaign, included the United Kingdom (UK) British Aerospace-146 (BAe-146), and the United States Department of Energy Gulfstream-1 (DoE-G1). The R/V *Ronald H. Brown* was also involved in the campaign. Throughout VOCALS, dedicated intercomparison periods took place between sampling platforms (also illustrated in Fig. 6). These consisted of level legs where aircraft and/or the R/V *Ron Brown* sampled the same air mass for a given amount of time, allowing direct comparison of instrument performance across platforms. More detailed descriptions of intercomparison periods can be found in Allen et al. (2010).

1.5.2 TAO cruise

Observations of marine aerosol were taken on board the NOAA R/V *Ka'imimoana* in August/September 2009. The ship left Pearl Harbor, Hawai'i on 24 August 2009, and transited to 9°N, 140°W. From there the ship serviced Tropical Atmosphere Ocean (TAO) buoys along 140°W from 9°N to 5°S. At that point (5°S, 140°W), the ship transited to the 125°W longitude line, and continued to service buoys from 8°S to 8°N, followed by a transit back to Pearl Harbor, finishing the campaign on the 25 September. Figure 8 shows the cruise track along with date labels.

1.5.3 IMPEX

The Intercontinental and Megacity Pollution Experiment (IMPEX) took place aboard the C-130 in April 2006, with 12 research flights from Seattle, WA over the Northeast Pacific Ocean. Most of these flights were designed to intercept transported

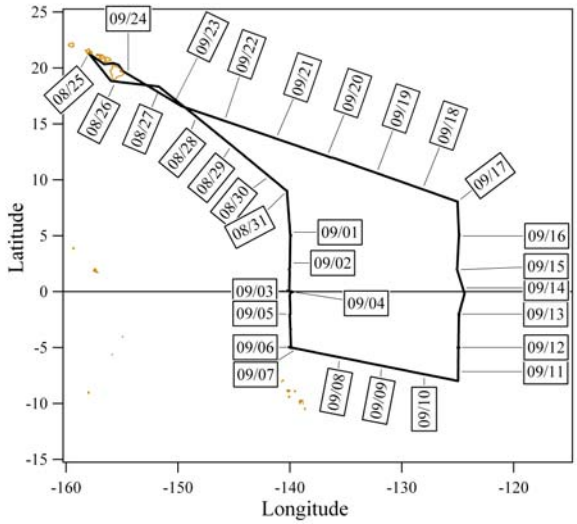

Figure 8. Cruise track for the TAO 2009 campaign on board the R/V *Kaiminmoana.*

Asian pollution layers as identified by chemical transport models (Dunlea et al., 2009) in between continents, namely between Asia and North America. Both the aging of aerosols and the structure of the pollution layers were investigated. For comparison against pollution aerosol, several instances of clean marine air were measured, even though clean aerosol was not the focus of the campaign.

2 Methods

Submicron aerosol was collected during VOCALS, the TAO cruise, and IMPEX. The mix of aerosol instrumentation varied for each study as described below.

2.1. Sampling inlets

On board the C-130 during both VOCALS and IMPEX, a Solid Diffuser Inlet (SDI) was used for the majority of sample collection. The inlet was kept isokinetic during sampling by adjusting flows as flight parameters (i.e., speed, altitude, etc.) changed. Inlet losses from the SDI are most severe for supermicron particles (Moore et

al., 2004). Moore et al. (2004) performed an inlet comparison study and found the SDI to effectively pass submicrometer (in the size range the AMS samples), as well as optically relevant coarse mode aerosol. McNaughton et al. (2007) tested University of Hawai'i's SDI against ground based measurements during the DC-8 Inlet Characterization Experiment (DICE) and found that submicrometer scattering agreed within 16%. The inlet efficiently transmits both dust and sea salt particles smaller than 4 μm (50% cut-off) in dry diameter. Aerosol is generally dry (desiccated) or heated by the time it is measured by any instrument used in the discussion of this thesis. Aerosol sampled by the aerosol mass spectrometer is not desiccated, but the drop in pressure from the inlet to the intermediate pressure chamber ensures aerosol is below a RH of 40% before it is ionized. Instrumentation was housed in two racks on board the C-130. A schematic of the instrument lay-out is provided in Fig. 9, which was optimized to minimize particle losses. However, due to differences in flow rates and paths additional losses may affect some instruments. Key instruments are described in more detail in the following sections.

On board the R/V *Ka'imimoana*, ¾ inch copper tubing (~30 meters) was used to bring air from the bow of the ship (forward of the stack) to the instruments housed inside the ship. The flow rate was approximately 40 liters per minute (lpm), and gravitational and diffusional losses for particles between 0.1 and 1 μm were estimated at < 5% (using Baron and Willeke, 2001). The sampling RH from the nephelometer was 56 ± 5 % (standard deviation) throughout the campaign.

Sample air was filtered through an upstream filter (Fig. 9) for at least five minutes, twice per 9-hour flight on the C-130, usually in the beginning and at the end of flights. Filter periods are run in order to confirm a leak-tight sampling system and calculate

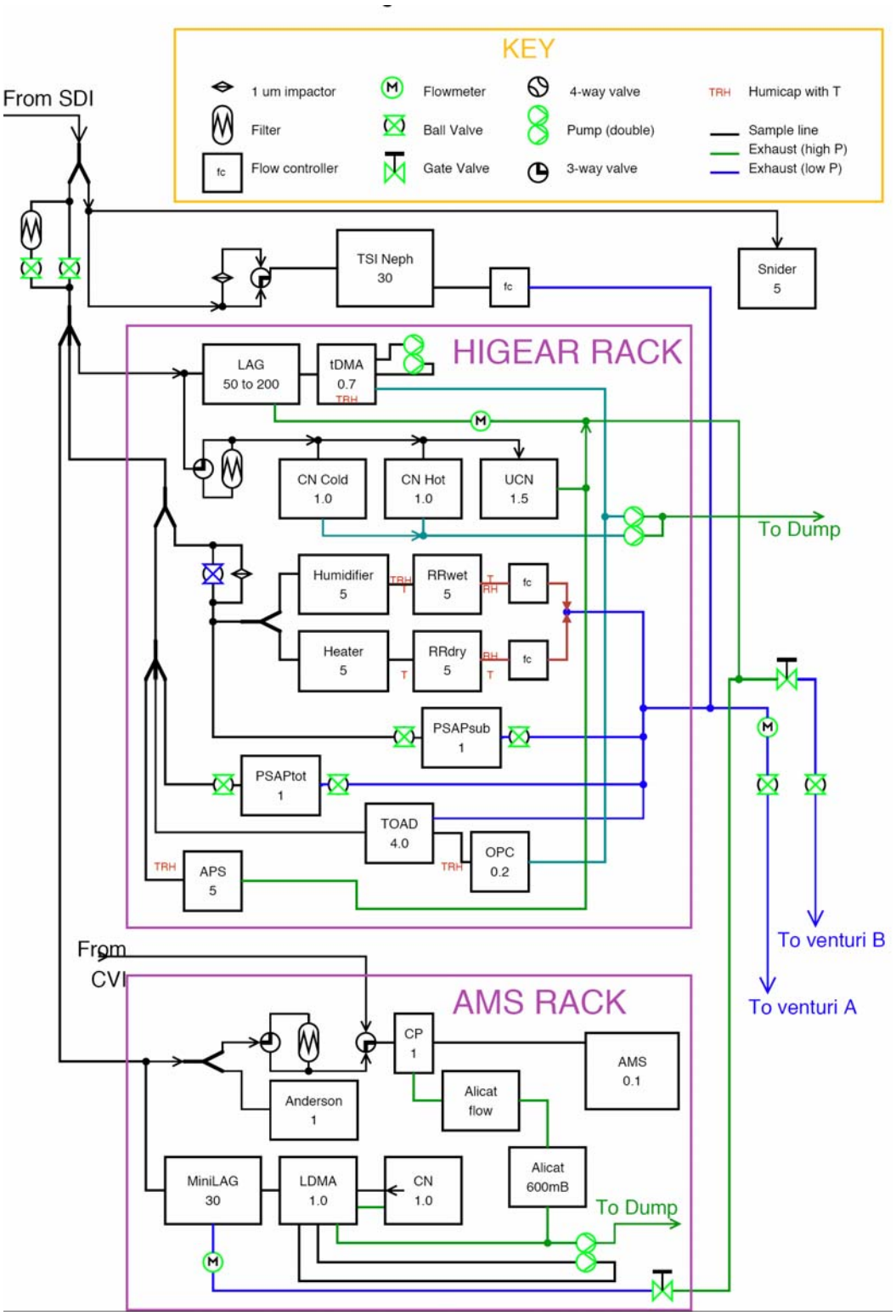

Figure 9. Schematic of the instrument racks on board the C-130. Flow rates are denoted in the instrument name box.

baselines and zeroing of instruments. Filter periods must be short on aircraft in order to minimize the loss of data during limited flight time. Filter periods during the cruise occurred once a day, and lasted at least 30 min.

2.2 Instrumentation

2.2.1 Aerosol Mass Spectrometer

During all three campaigns, non-refractory chemical composition of submicron aerosols was determined using an Aerodyne High Resolution Time of Flight Mass Spectrometer (HR-ToF-AMS), see Fig. 10 for a schematic of the instrument. Non-refractory refers to particles which volatilize at the temperature of the AMS heater

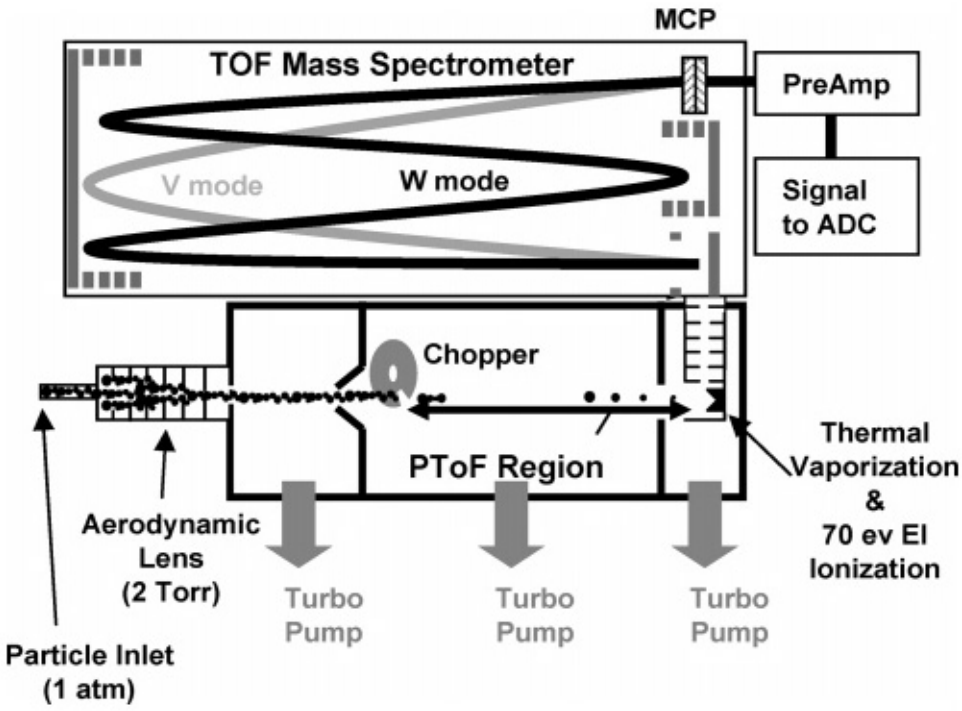

Figure 10. Schematic of the Aerodyne High Resolution – Time of Flight – Aerosol Mass Spectrometer.

(~600°C). The HR- ToF-AMS (~1.4 $cm^3 s^{-1}$ flow rate) uses an aerodynamic lens assembly to focus 35 nm - 1μm vacuum aerodynamic diameter particles onto a 600°C heated surface (Zhang et al., 2002; Zhang et al., 2004). Vacuum aerodynamic diameter is the ratio between the physical diameter of a particle and the particle density. Particles are evaporated off the heater, ionized by electron impaction (70 eV), and mass analyzed by ToF-MS.

The AMS was typically operated in high-sensitivity mode (V-mode), though on the ship and occasionally during VOCALS, the instrument was operated in a high resolution mode (W-mode), which offers more detailed chemical composition of ion fragments (at the cost of a 50 fold increase in detection limit). All data shown in the current study is V-mode, and is a subtraction of open sampling versus closed periods. A chopper wheel (Fig. 10) alternately blocks and unblocks the particle beam, permitting particles to hit the heater and be detected. The difference in the open minus closed signals is attributed to the particles. A detailed description of the instrument and its operation is given in DeCarlo et al. (2006) and Canagaratna et al (2007).

Typical detection limits for one-minute averaged V-mode data have been reported as < 0.04 μg m^{-3} for all chemical species (SO_4, Org, nitrate (NO_3), and ammonium (NH_4)) (DeCarlo et al., 2006). However, these detection limits were derived from ground-based experiments. Aircraft-based AMS mean detection limit measurements are typically 2-5 times higher due to higher background because the instrument has to be turned off between flights. When the turbo pumps on the AMS are tuned off between flights, material builds up on the inside of the vacuum chamber. For several hours after the AMS turns on, this material is driven out of the system by the heater. For some material, e.g.

Org, this process may take several hours. Therefore, at the beginning of the flight there is a higher Org background which contributes to more noise and a higher detection limit, particularly in clean areas with a small signal superimposed on a large background, see Fig. 11. Detection limits for our campaigns were defined as twice the standard deviation of the species signal during a filter period. For example, during VOCALS the detection limit varied depending on the duration of AMS operation over a flight, and with lower detection limits reached after several hours. The lowest detection limit for one minute averaged OM was calculated to be 0.06 μg m^{-3}, while for SO_4 it was 0.013 μg m^{-3}.

The overall ability of the AMS to transmit and detect particles is termed the collection efficiency (CE) and takes into account the transmission efficiency of the aerodynamic lens, the loss of transmission because of non-sphericity, and the efficiency with which a vaporized particle is detected (Huffman et al., 2005). The CE of the AMS

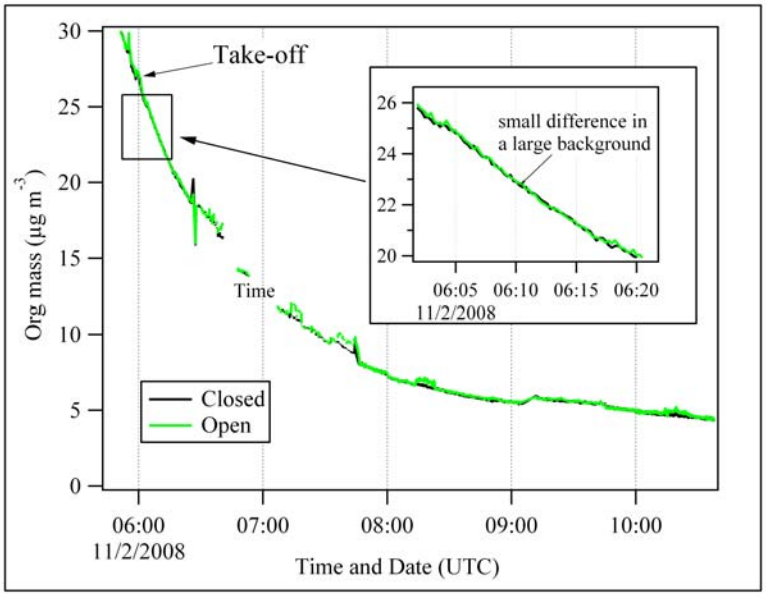

Figure 11. Differences in open versus closed Org mass signal over the period of a flight (VOCALS, Research Flight 8, 2 November 2008).

for the inorganic ions was estimated by comparing the molar ratio of NH_4 to SO_4 to determine the acidity of the aerosol. Because it is less likely to bounce off the heater and thus not be detected, acidic aerosol (i.e., lower NH_4/SO_4 molar ratio) is collected more efficiently than neutralized aerosol (Drewnick et al., 2003). The CE correction factor was determined by finding the NH_4/SO_4 over the desired collection time, and assuming CE varies linearly (from 50 to 100%) as the ratio of NH_4/SO_4 decreases from 1 to 0 (Matthew et al., 2008). Anytime the NH_4/SO_4 ratio is above 1, the CE is assumed to be 50%.

The ionization efficiency (IE) calibration determines the ionization efficiency of ammonium nitrate (NH_4NO_3). The quantification of all non-refractory AMS components (SO_4, NH_4, and Org) is based on the linearity of the IE of NO_3 (Jimenez, 2010). These are typically done in the field using Brute-Force Single Particle Mode (BFSP). IE calibrations were run once a week (every three flights) throughout VOCALS using generated NH_4NO_3 aerosol. An IE calibration was run at the beginning of the TAO 2009 cruise. However, the chopper wheel stopped working half way through the campaign, and therefore no additional IE calibrations were feasible.

Processing of the AMS data was done using the standard AMS data analysis software (SQUIRREL v.1.48C and PIKA v.1.07B, Sueper, 2010) within Igor Pro 6 (Wavemetrics, Lake Oswego, OR). The fragmentation table in SQUIRREL was adjusted to give zero Org mass concentrations during filter periods. The description of specific adjustments can be found in Appendix A.

2.2.2 Single Particle Soot Photometer

During VOCALS and IMPEX a single particle soot photometer (SP2) was also used to measure BC particle number and mass for sizes between about 0.11 - 0.5 μm.

This instrument uses the fact that BC absorbs laser energy at 1060 nm and is heated rapidly to incandesce when it emits light which is captured by a detector. As BC is the only significant absorber, this allows for fast single particle quantification of BC. The detector configuration and triggering method were set up according to the manufacturer (Droplet Measurement Technolgoies (DMT)) as described in Stephens et al. (2003) and Schwarz et al. (2006)). The detectors were photomultiplier tubes (PMTs) for two incandescence channels (broad/narrow) and Si-avalanche photodiodes (APDs) for two scattering channels (see Fig. 12 for a schematic of the SP2). During VOCALS, events were triggered from the broad incandescence channel.

The incandescence channels response was converted to refractory BC mass using a calibration curve generated with laboratory black carbon (Aquadag), sized using a long differential mobility analyzer (LDMA, described in Sect. 2.2.3). The effective density of Aquadag was generated according to Moteki and Kondo (2010). While it is true that a significant number of BC particles may exist below the limit of SP2 detection, in the case of remote aged atmospheric soot we generally find the SP2 misses less than 10% of the ambient BC mass. If this were significant we would expect a positive intercept for regression of absorption against SP2 BC mass but this is not what we find (e.g., McNaughton et al., 2011). It should be mentioned that recently it has been shown by Gysel et al. (2011) that the effective density of Aquadag is lower, by about 35%, than Moteki and Kondo (2010) find. This could result in our BC measurements reported here being too high. These results are new enough that they have been regarded as tentative (still in review), and therefore we have not corrected our results as it does not affect the logic of our current study.

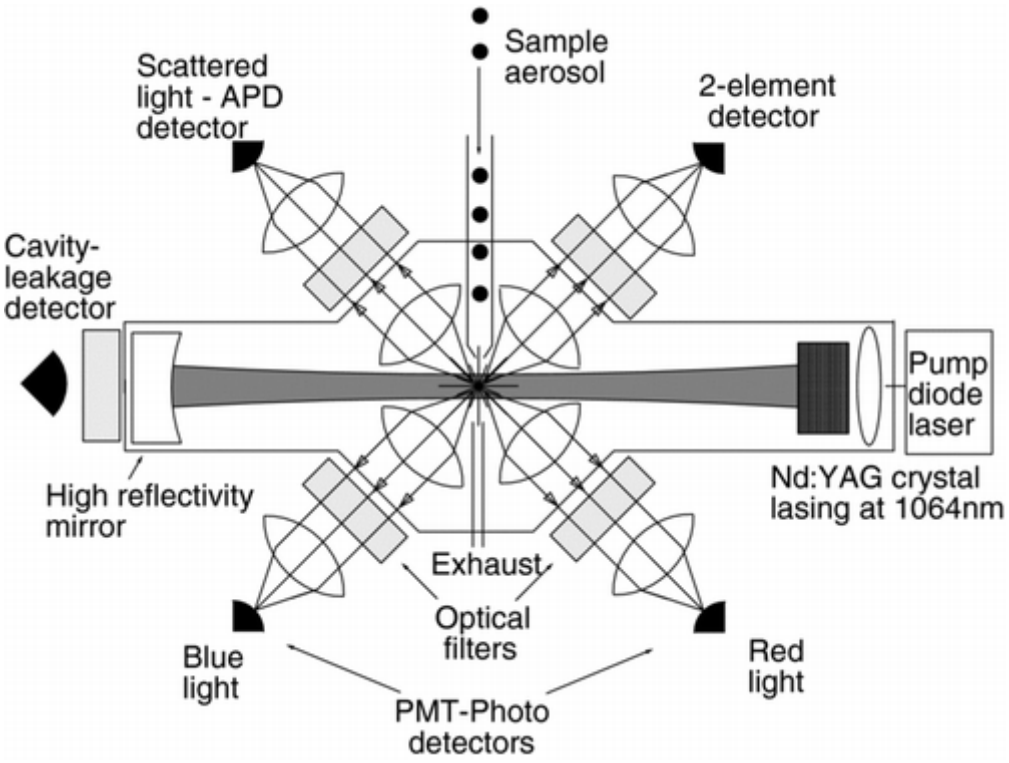

Figure 12. Schematic of the SP2 used during VOCALS. In place of the blue and red detectors, we used narrow and wide band PMTs. Source: Schwarz et al., 2010.

2.2.3 Other aerosol and gas measurements

Among many other aerosol optical and physical measurements taken on board the C-130 during VOCALS, particle concentrations were monitored with condensation nuclei (CN) counters (TSI 3010). Two CN counters were operated in parallel; one with an inlet heated to 360°C. Non-volatile CN (CNhot) refers to those particles which do not volatilize at 360°C, i.e., sea-salt and soot, the latter as a proxy for pollution. An Optical Particle Counter (OPC), LAS-X with modified electronics, was also operated using a heated inlet which cycled between non-heated, 150, 300, and 400°C, and yielded size distributions of the aerosol (Clarke, 1991). Figure 13 shows the differences in particle volume distributions measured by the OPC for non-heated and heated (400°C) aerosol. The volume distributions in Fig. 13 represent a clean MBL leg during VOCALS. The

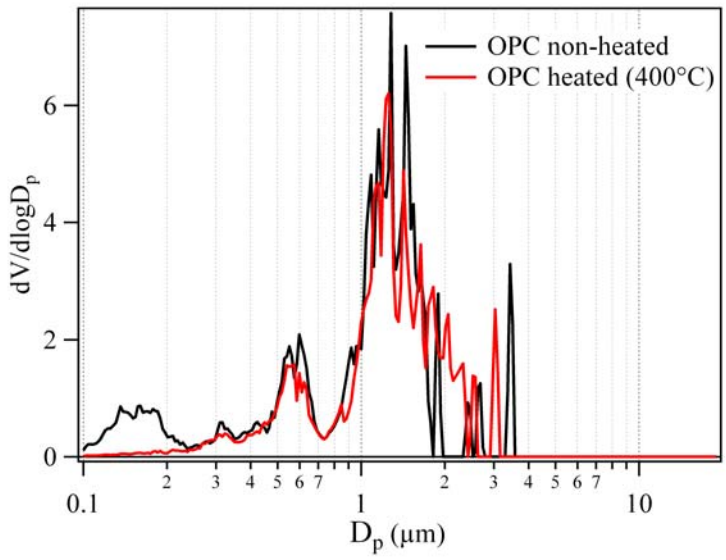

Figure 13. Heated and non-heated volume distributions measured by the OPC during a VOCALS clean MBL leg (Research Flight 11, 9 November 2008, 15:25-15:35 UTC). Subtraction of the red curve (heated distribution) from the black curve (non-heated distribution) gives the total non-refractory volume.

difference in the non-heated and heated distributions (e.g., black curve in Fig. 13 minus the red curve) reflects the amount of non-refractory (volatile) material present.

A long differential mobility analyzer (LDMA) model TSI 3934 with modified flow control, electronics, and data acquisition was used to acquire size distributions in the 10-500 nm range. The LDMA was operated in a scanning mode, with an up-scan time of 60 seconds. The LDMA drew air from an all-aluminum lagged aerosol grab (LAG) chamber, which is open for ~20 s every 2 minutes (Clarke et al., 1998). The inversions were done using a LabView program written by J. Zhou and are described in his dissertation (Zhou, 2001). Also on board was a three-wavelength TSI nephelometer (model 3563) used to measure both submicron and total particle scattering. Figure 14 shows a real aerosol size distribution measured during a clean VOCALS leg, using a combination of instrument measurements. We also flew an Aerodynamic Particle Sizer (APS), but since it measures

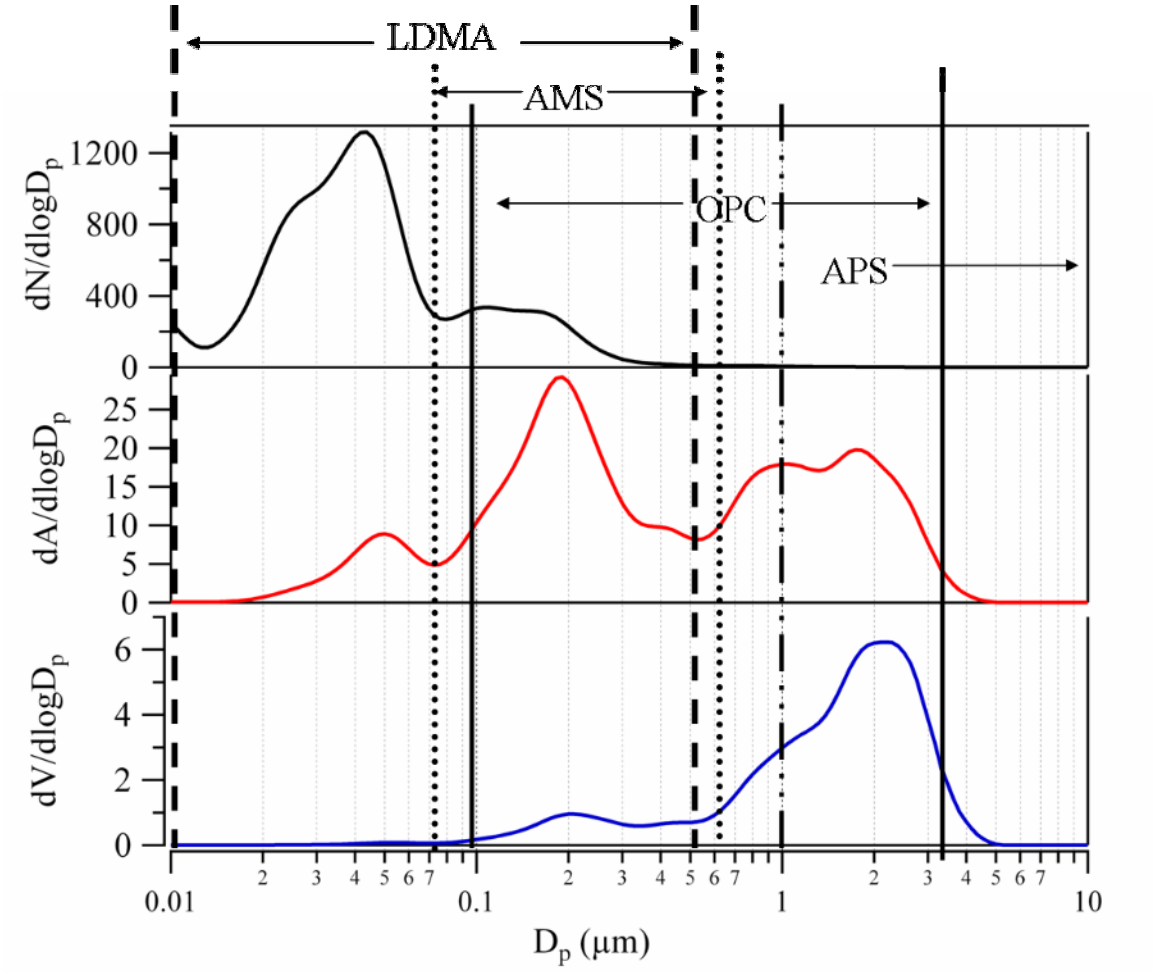

Figure 14. Marine aerosol size, area, and volume distributions. The size ranges of the different aerosol instruments are indicated. Average distributions from VOCALS Research Flight 11, 9 November 2008, 15:25-15:35 UTC.

supermicron particles, and the focus of the current study is on submicron particles, a description of that instrument will not be provided.

CO was measured on the C-130 using a vacuum UV resonance fluorescence instrument similar to that of Gerbig et al. (1999). Precision is reported as ± 3 ppb and accuracy as better than 10 % for a mixing ratio of 100 ppb (Pfister, 2010).

The instrumentation suite aboard the *Ka'imimoana* included the AMS, CN counters (heated and unheated), nephelometer, and LDMA.

3 Results

3.1 AMS results

Our AMS results were compared against other VOCALS platforms, but were concentrated on intercomparisons with the BAe-146 since they flew an identical instrument to ours. AMS data across all platforms was found to contain no systematic sampling biases, and mean quantities from intercomparison runs agreed within one standard deviation (Allen et al., 2010). The comparison between the BAe-146 and C-130 AMS data showed agreement within 20% for the absolute values of Org and SO_4, and showed less than 6% disagreement in the Org/SO_4 ratio.

However, the agreement between the *Ron Brown* and C-130 AMS data during intercomparison periods was not as consistent. The AMS on board the Ron Brown was an Aerodyne Quadrupole AMS (Q-AMS), with significantly higher detection limits for Org (0.16 μg m^{-3}) than the ToF-AMS operated aboard the aircraft (~ 0.06 μg m^{-3}). Therefore, when intercomparisons were conducted during periods with Org concentrations near the detection limit of the Q-AMS, the discrepancies between platforms were worse than during periods of elevated Org concentrations. During the latter periods, comparison between the C-130 and Ron Brown AMS Org/SO_4 ratio was within the expected uncertainties of the instruments.

Before using AMS data from the C-130 in the analysis it was examined for consistency with other C-130 data sets. In order to test AMS collection efficiency and determine whether or not significant particle losses occurred, submicron non-refractory AMS mass was compared to submicron aerosol volume determined from size distributions measured by the LDMA, assuming a particle density of 1.7 g cm^{-3} for dry

sulfate. Although OM has been shown to have a lower density than that of SO_4 when sampled by the AMS (Cross et al., 2007), given the high mass fraction of SO_4 (> 75%) and the low contribution of Org (< 10 %) in the VOCALS and TAO regions (Allen et al., 2010; Hawkins et al., 2010; current study), an assumption of 1.7 g cm^{-3} was made for the purposes of this analysis. This provided an independent assessment of potential particle losses by the AMS. Figure 15 shows a plot of AMS mass and LDMA mass for the VOCALS marine boundary layer (MBL) that yields a linear regression equation with a slope of 0.65, R^2=0.68, suggesting that the AMS was under-sampling submicron aerosol compared to the LDMA ($LDMA_{before}$).

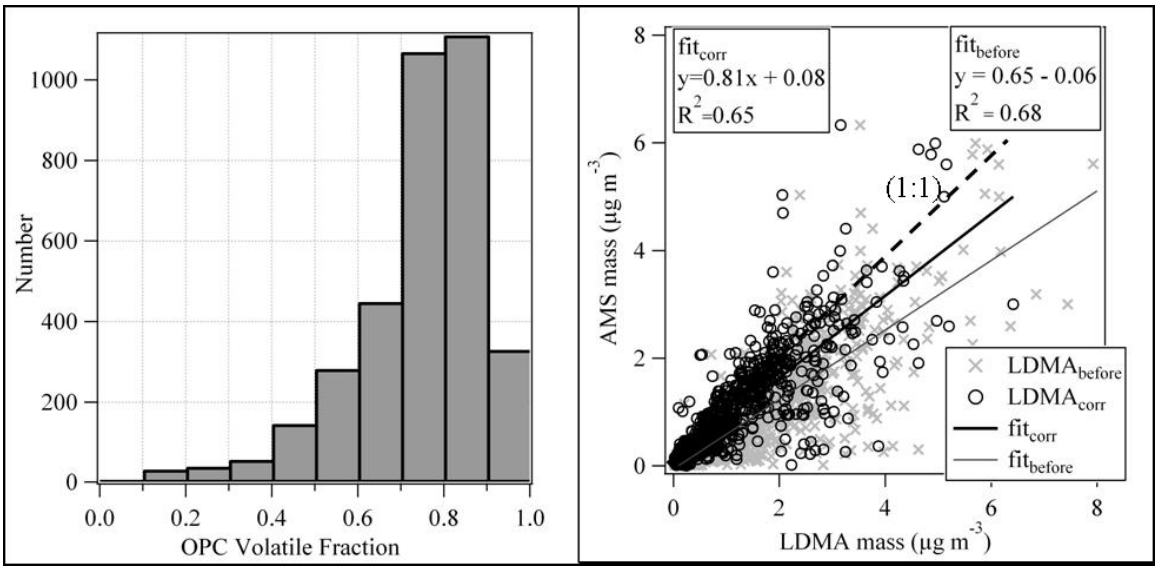

Figure 15. (Left) Histogram of the volatile fraction established from the OPC. (Right) Relationship between LDMA volatile mass and AMS mass for the VOCALS MBL before and after the non-volatile correction factor.

However, the LDMA distributions can include refractory mass, (e.g., sea-salt, dust, soot, and/or refractory Org) not detected by the AMS. Also, sodium sulfate

(Na_2SO_4) resulting from reaction between sulfuric acid (H_2SO_4) and sodium chloride (NaCl) is likely to be significant in aged aerosol, and may or may not be sampled efficiently by the AMS. Consequently, LDMA volumes were corrected for non-volatile mass determined independently by the OPC. The volatile mass from the OPC was calculated as the difference between the non-heated mass (M1) and the mass that remains at 400°C (M4) (e.g., Fig. 13) over the same size bins as the LDMA (~10-500 nm) (overlap region between AMS, OPC, and LDMA as shown in Fig. 14). The fraction of volatile mass (Vol) was then calculated using Vol = (M1 - M4)/M1. A histogram of the OPC volatile fraction is shown in Fig. 15 as well. This measured OPC volatile mass fraction was multiplied by the measured LDMA mass over the same time periods (approximately 90 s) in order to estimate only the volatile LDMA mass. The resulting estimated LDMA volatile mass was then compared with the AMS, and is plotted in Fig. 15 as black circles over the uncorrected data in grey. After this correction for refractory mass, the slope of the linear regression between the LDMA and AMS improved to 0.81, R^2=0.65, indicating significantly better quantitative agreement with the non-refractory aerosol component. The comparison between LDMA, OPC, and AMS is not perfect, and is complicated by incommensurate time scales which make direct comparisons difficult. It is relevant to note that the AMS and OPC data are averaged over 90 s timescales in order to compare with the LDMA, and even then the AMS spends half the sampling time in a closed mode. The LDMA size distributions represent a 20 s grab sample that is then scanned over a 60 s period. Selecting only periods of stable conditions might reduce noise, but would not affect the overall slope. Also, while we assumed a CE of 0.5 was a reasonable approximation to the results of Matthew et al. (2008) and Middlebrook et al.

(2011), their mean CE was ~0.43. Correcting this, plus our possible overestimate of particle density of 1.7 g cm^{-3}, could increase our estimate of overall AMS efficiency from 0.81 to >0.94 compared to the LDMA.

Average mass spectra for clean periods during VOCALS and TAO are shown in Fig. 16. Note the noisier data in VOCALS due to high Org background and inability to average over longer periods of time on the aircraft. The red SO_4 peaks dominate the mass spectra (note log scale on the y-axis), and there are few Org peaks above the noise of the instrument (height of the black peaks in Fig. 16) illustrating the low values of Org mass, near the detection limit of the instrument, encountered during VOCALS. The largest Org peaks occur at m/z 27 (C_2H_3), 44 (CO_2), 45 ($^{13}CO_2$, CO_2H), and 56 (C_4H_8).

3.2 VOCALS AMS results

Table 2 shows the average concentrations for SO_4, Org, NO_3, and NH_4 for VOCALS and TAO 2009, as well as average BC mass and CO for VOCALS. In addition, average values of these aerosol constituents and the average Org/SO_4 ratio from several previous clean marine investigations are shown for comparison. Uncertainties representing the natural variability of the system are also shown for the current study, and those earlier studies where uncertainties were reported. Our VOCALS data is averaged based on three criteria. The first is simply campaign-averaged MBL, the second is the nominally clean MBL, with data restricted to BC mass less than 4.5 ng m^{-3} and CO less than 61 ppb, values representative of background conditions in the SEP, and the best direct comparison between clean cases in the SEP and the North Atlantic (Mace Head). Finally, our criteria for the natural MBL as determined during this study, and discussed in Sect. 4.1.

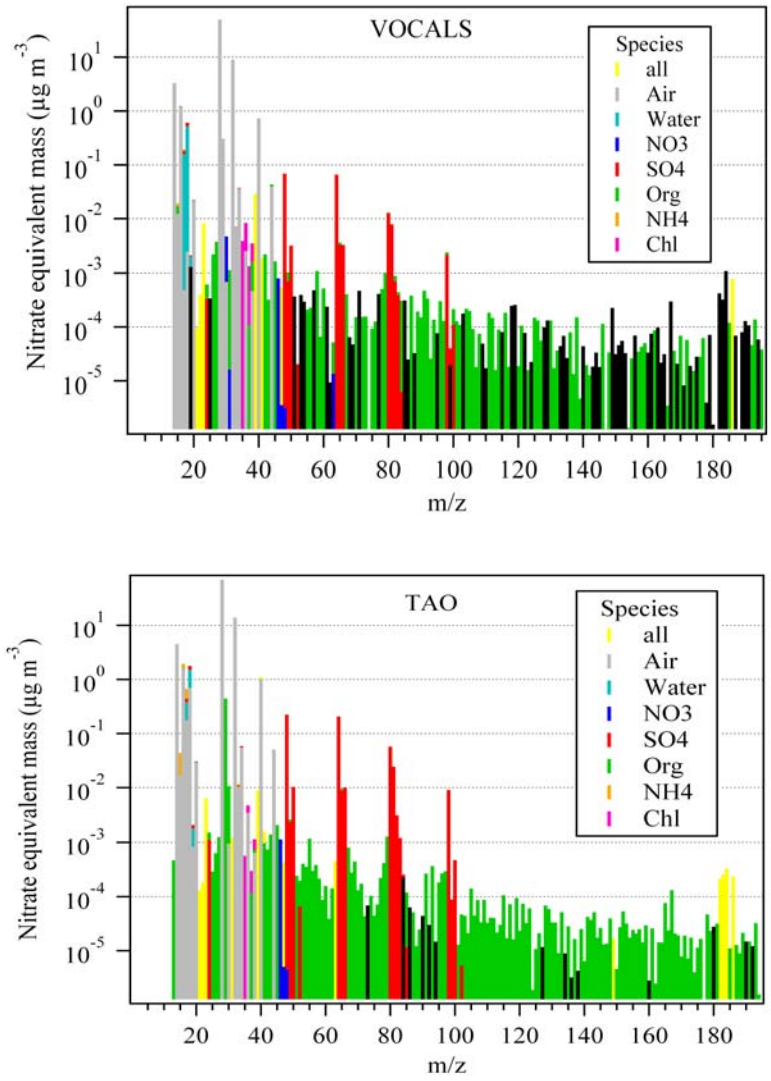

Figure 16. Average mass spectra results from clean periods during VOCALS (Research Flight 11, 9 November 2008, 15:25-15:35 UTC) and TAO (5 September 2009, 3:00-15:00 UTC). Black peaks indicate negative ion fragments and reflect instrument noise.

Pie charts in Fig. 17 illustrate the relative composition of clean submicron non-refractory mass during VOCALS compared to findings from previous investigations.

Table 2. Average submicron mass concentrations for major aerosol constituents from current and previous investigations of "clean" marine submicron aerosol[a].

Where	When	SO4	Org	NH4	NO3	BC	CO	Org/ SO_4	Criteria[b]
North Pacific, Trindad Head, California[c]	Apr-May 02	0.93	0.38	0.2	0.09			0.41	2, 5, 8,9
North Pacific, Ocean Station Papa (50.0° N, 145.0° W)[d]	Jul 02	0.74±0.04	0.3±0.1	0.15±0.1	0.03±0.01			0.41	2
North Atlantic, Mace Head, Ireland[e]	Apr-Jun, Sep-Oct 02	0.26±0.04	0.91±0.12	0.06	0.02±0.01	0.02		3.5	1, 2, 7
Ace-Asia, R/V Ron Brown[f]	Apr 02	0.72±0.58	0.39±0.15	0.17±0.16	0.01±0.01			0.54	2
North Pacific, Seattle, Washington[g]	Apr 06	0.52	0.15	0.16	0.02			0.2	
Southeast Pacific, R/V Ron Brown[h]	Oct-Nov 08	0.67	0.1	NA	NA			0.15	6, 7
South Atlantic, R/V Marion Dufresne (20–60°S, 70° W–60° E)[i]	Jan-Mar 07								
"Clean Atlantic"		0.18	0.03	0.06	<0.01			0.17	2
"Antarctic"		0.31	0.02	0.05	0.01			0.06	
"Bloom"		0.21	0.32	0.07	0.02			1.5	
Southeast Pacific, VOCALS[j]		**0.52±0.65**	**0.10±0.20**	**0.06±0.12**	**< 0.01**	**0.01±0.02**	**60.4± 12.5**	**0.19**	**3, 4**
clean MBL current study[k]	**Oct-Nov 08**	**0.17±0.12**	**0.02±0.02**	**< 0.01**	**< 0.01**	**0.002±0.001**	**57.1±6.8**	**0.12**	
natural MBL current study[l]		**0.20±0.11**	**0.02±0.02**	**< 0.01**	**< 0.01**	**<0.001**	**56.8±5.6**	**0 .1**	
Central Pacific, TAO[j,m]	**Aug-Sep 09**	**0.79±056**	**0.08 ±0.07**	**0.10±0.10**	**<0.01**			**0.1**	

Note: Uncertainty ranges are included, when reported in previous studies. For the current study, the uncertainties shown represent the natural variability in the environment, as these overwhelm the uncertainties due to the instrument and sampling methods.

[a]All concentrations are in µg m^{-3} except BC (ng m^{-3}) and CO (ppb); [b]Abbreviations for clean air criteria: 1=Clean air sector, 2=Air Mass Back Trajectories, 3=BC threshold, 4=CO threshold, 5=correlation with volatile organic carbon (MTBE), 6=radon, 7=particle number concentration, 8=increase in organic accumulation mode mean diameter, 9=Volatile Organic Carbon (VOC) tracers; [c]Allen et al., 2004; [d]Phinney et al., 2006; [e]Cavalli et al., 2004, [f]Quinn et al., 2004, [g]IMPEX, [h]Hawkins et al., 2010, [i]Zorn et al., 2008; [j]Current study, [k]Data restricted to BC < 4.5 ng m^{-3} , CO < 61 ppb, [l]Data restricted to BC < 1.8 ng m^{-3} , CO < 56 ppb, [m]CN < 700 cm^{-3}

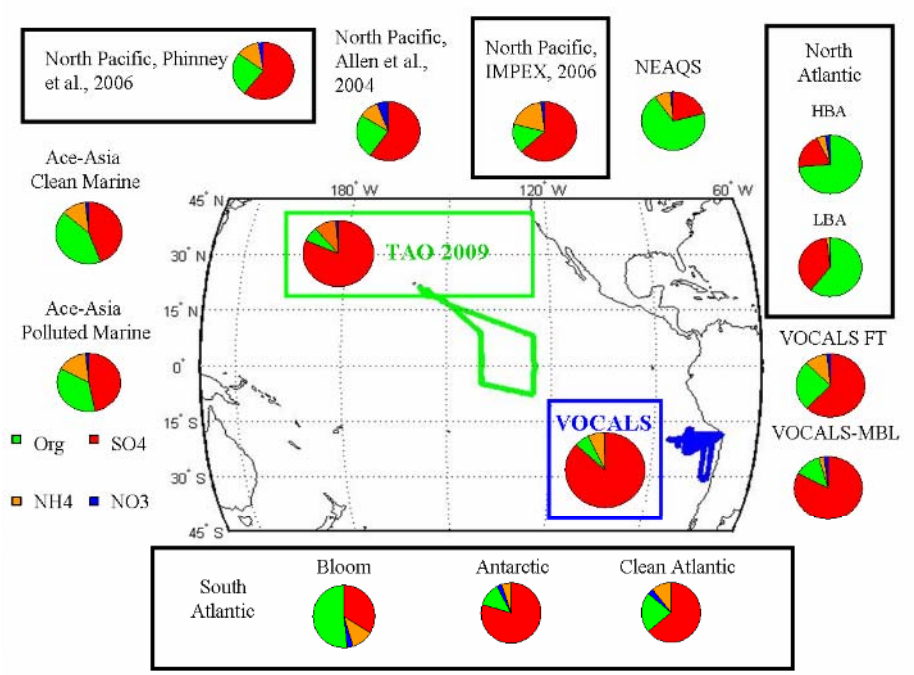

Figure 17. Study region for VOCALS (blue) and TAO 2009 cruise (green). Pie charts indicate relative contributions of submicron non-refractory species. All studies are of marine boundary layer aerosols, with the exception of the VOCALS Free Troposphere data (FT). Studies in bold boxes indicate those which focus on "clean" marine aerosol, (i.e., based upon various approaches to minimize continental influence). NEAQS=New England Air Quality Study, HBA=High Biological Activity, LBA=Low Biological Activity. Ace-Asia and NEAQS data adapted from Quinn and Bates, 2003, North Atlantic from O'Dowd and de Leeuw, 2007, and South Atlantic from Zorn et al., 2008.

3.3 TAO AMS results

Data from the TAO 2009 cruise had to be screened for ship contamination. Periods influenced by the ship's plume were removed from the AMS data based upon exceeding a criteria of 700 cm^{-3} for CNhot and 15 Mm^{-1} for submicron scattering values from the TSI nephelometer. Next, CNhot (1 Hz data) was smoothed with a 12-point median filter. The smoothed data was subtracted from the raw data in order to capture any rapid changes in the concentration possibly related to stack contamination. Any data point where the difference in raw and smoothed data, on a one second time scale, was greater than a concentration of 200 particles cm^{-3} was removed. After this screening the

same CE assessment employed for the VOCALS data was applied to the TAO data. The resulting average concentration of SO_4 was 0.85 μg m^{-3}, while Org was 0.07 μg m^{-3}. NH_4 concentrations averaged 0.11 μg m^{-3}.

During the TAO cruise neither CO nor BC measurements were made, making it more difficult to identify air influenced by continental pollution. However, a plot of Org vs. SO_4 for the entire cruise (100 minute averaged data), overlaid by VOCALS data (10 minute, or leg-averaged, data), shows a considerable fraction of the measurements lie on or near to a line with a slope ~0.1 (TAO and VOC, Fig. 18). VOCALS FT data (VOC FT), where the Org/SO_4 is significantly higher, is also plotted and reveals the potential to increase MBL values of Org/SO_4 through entrainment.

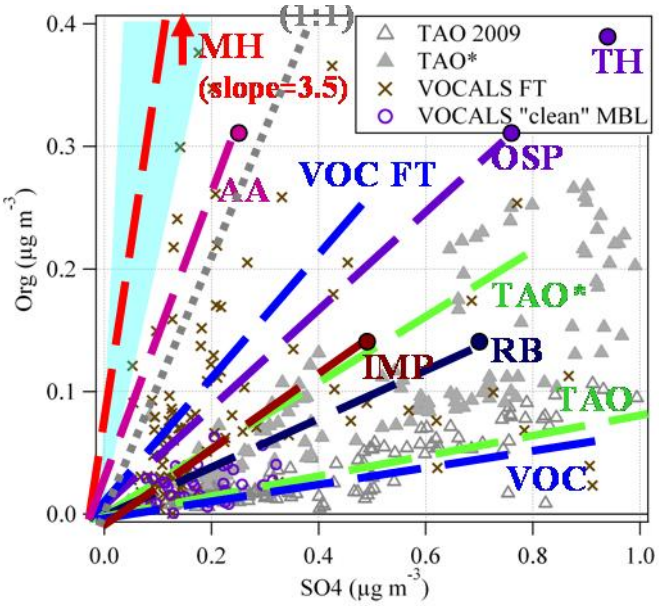

Figure 18. AMS organics (Org) versus sulfate (SO4) during TAO 2009 cruise, VOCALS "clean" MBL(VOC), and VOCALS FT. Also shown are approximate implicit slopes for the Org/SO4 relationship from Trinidad Head (TH), Mace Head (MH), Ace-Asia (AA), IMPEX (IMP), Ocean Station Papa (OSP), and VOCALS Ron Brown (RB). Average reported clean values are shown as circles, while the dashed lines indicate the implicit slope. Excursions from the TAO average Org/SO4 of 0.08 are indicated as TAO*. A range of biomass burning Org/SO4 ratios are indicated by the blue triangle.

A time series of TAO cruise data for SO_4, Org, NH_4 and NO_3 are shown in Fig. 19, along with the time series of Org/SO_4. Figure 19 also includes the cruise track with date labels, rain events, and wind direction indicated. The excursions from the average Org/SO_4 ratio are pronounced along the easternmost leg of the cruise, along 125°W from 8°S to 5°N, where Org concentrations increase gradually from 0.07 μg m^{-3} at the southern end of the cruise track, to 0.17 μg m^{-3} near the equator. As the ship moved north after 15 September, and north of the Intertropical Convergence Zone (ITCZ), the Org/SO_4 ratio decreased to values below 0.1, typical of those observed elsewhere during the cruise, while the absolute value of Org also decreased back to concentrations typical of the cruise average 0.07 μg m^{-3}. These excursions from the TAO cruise-average ratio of 0.08 are indicated by TAO* in Fig. 18 and the mean value indicated as a pie chart in Fig. 17. From 12 September to 14 September (indicated in the black circle in Fig 19), there is a

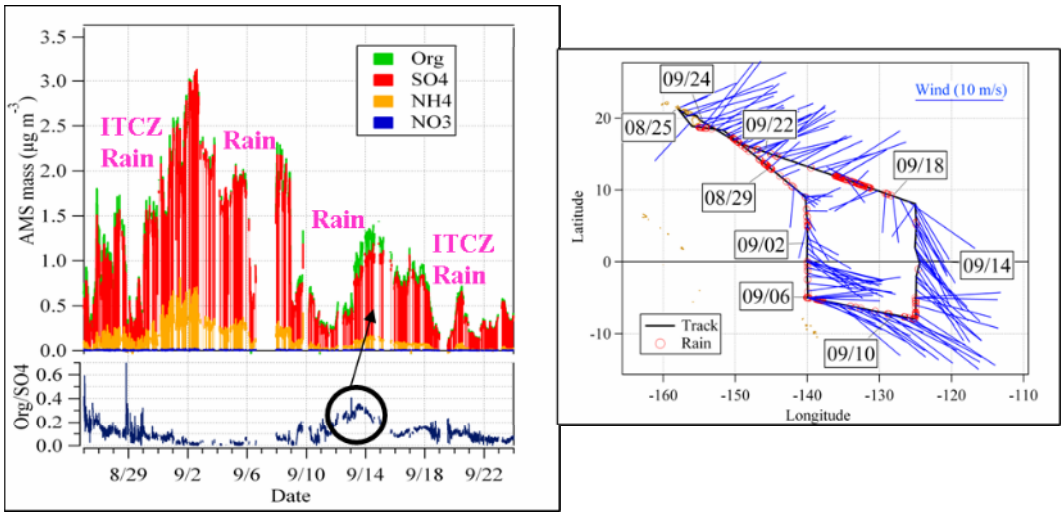

Figure 19. (Left) Time series of AMS Org, SO_4, NH_4, NO_3 and Org/SO_4 for TAO 2009 cruise. Dark circle and arrows indicate the increase in both Org/SO_4 ratio and absolute Org values along the eastern leg of the cruise track. (Right) Cruise track with date tags, rain events, and wind direction (blue lines pointing into the wind).

relatively consistent Org/SO_4 ratio during a factor of 5 change in total aerosol concentration,suggesting SO_4 is not preferentially removed by precipitation and this removal mechanism does not bias the ratio.

The AMS was operated in both V and W modes during the cruise, cycling between the two modes every one and four minutes, respectively. When cycling between the two modes, ten minute averages include only two minutes of V-mode data, compared to 10 minutes of data when operating solely in V-mode. Due to problems with a variable air beam when operating in W-mode, we operated the instrument only in V-mode after 10 September. Since the current study focuses on V-mode data exclusively, the data is therefore noisier before 10 September than after.

4 Discussion

4.1 Determination of clean air criteria in the SEP

Particulate species, such as BC and Org, can be scavenged from the atmosphere by precipitation but CO is not. CO is only slowly removed by reaction with OH with an e-folding time of about 1-2 months (Jaffe et al., 1997) in the tropics and over a year in high latitudes during the winter (Staudt et al., 2001). These properties allow use of gas phase CO and aerosol phase BC as a tool for identifying combustion influences and for establishing clean marine criteria. Here they are also combined with AMBTs to isolate a marine-source contribution of Org to the remote marine atmosphere.

The Southern Hemisphere has lower background levels of CO and BC than the Northern Hemisphere, where there is more land mass, more human population, and more combustion sources. This should make it easier to find instances where continental organics are dwarfed by marine sources. Histograms of CO in the VOCALS MBL show

a division between two modes at about 61 ppb (Fig. 20). The lower CO mode appears to be related to trajectories coming from the Southern Ocean, while the higher CO mode correspond to MBL trajectories that often appear to contact the South American continent, perhaps bringing air masses influenced by the Santiago region over the SEP. The lower CO mode (CO < 61 ppb) was therefore chosen as representative of background concentrations in this region. Also, a plot of CO versus BC indicated that when BC goes to zero (no pollution), CO values range from ~53-61 ppb (Fig. 20), another indication that CO values near 61ppb represent the upper limit of background conditions in the SEP. A BC concentration of 4.5 ng m^{-3} was established because it represents the average BC concentration (actual average was 3.66 ± 4.26 ng m^{-3}) in the low CO mode (CO < 61 ppb). Therefore, these concentrations were taken as background conditions for the SEP, and represent data that can be directly compared with that from Mace Head.

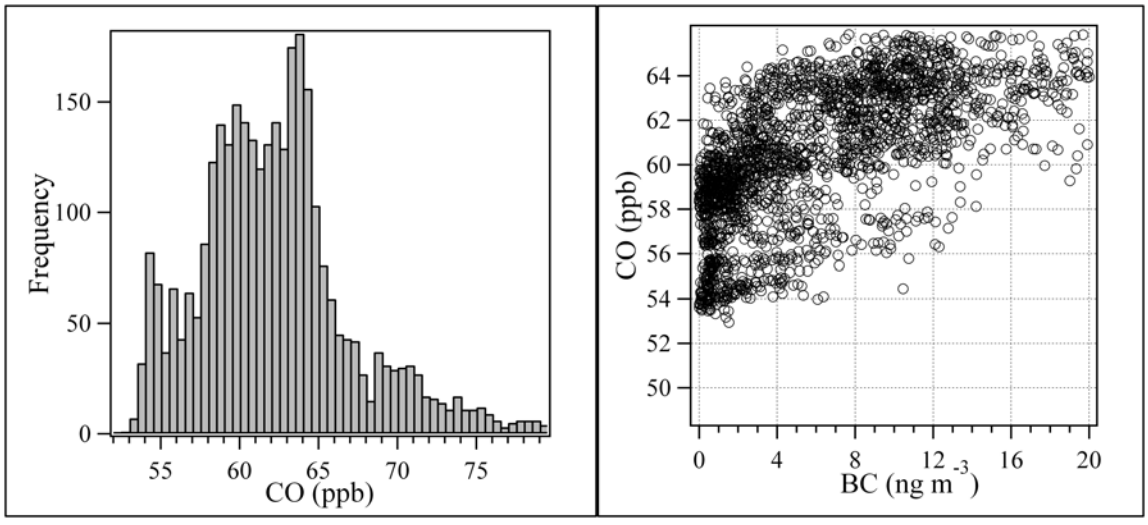

Figure 20. (Left) Histogram of CO in the VOCALS MBL; (Right) CO versus BC at low BC mass.

Org vs BC and SO_4 vs BC, as well as CO in the VOCALS MBL are plotted in Fig. 21. Figure 21a shows Org vs BC and Fig. 21b shows the SO_4 vs BC relationships for the free troposphere (FT) and MBL, all colored by CO. Above cloud air in the FT often has higher concentrations of Org, BC, and CO than below cloud, but lower SO_4 concentrations. Entrainment evident in this region (Bretherton et al., 2010) would therefore raise concentrations of Org and BC in the MBL while lowering SO_4 by dilution. Furthermore, the range of relationships evident between OC and BC in the FT in Fig. 21a suggest the involvement of variable sources and aerosol removal processes. Figure 22 illustrates the potential differences in pollution sources in the FT. This figure depicts two

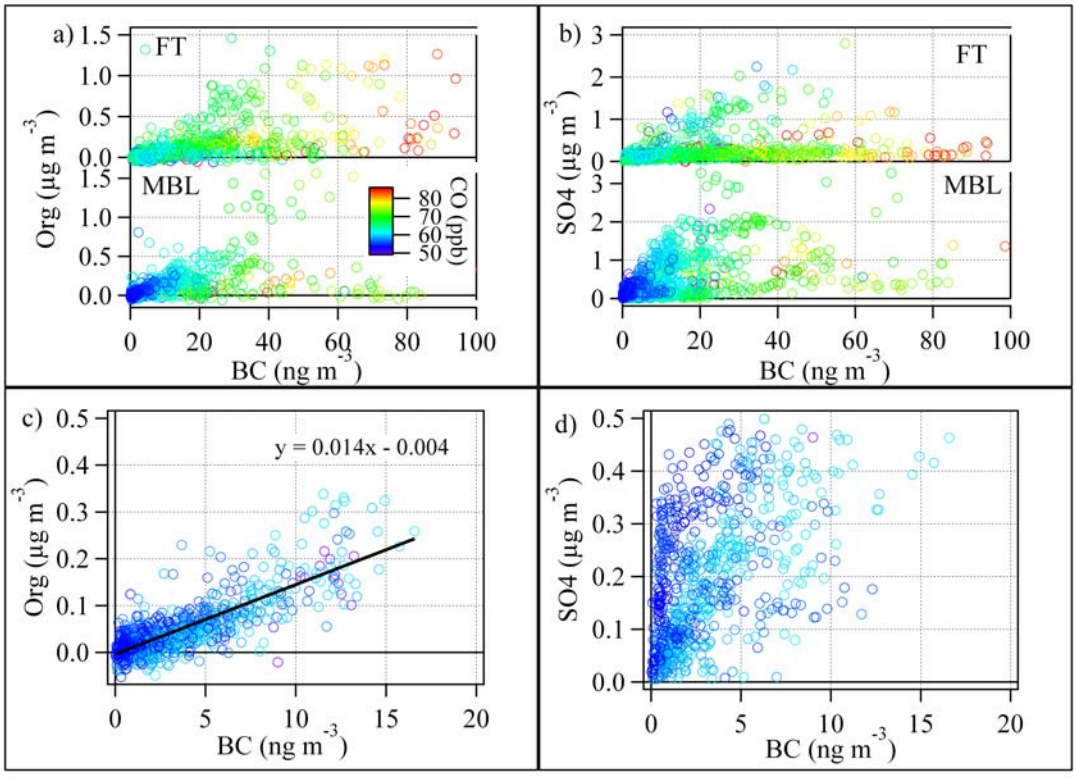

Figure 21. **(a)** Org vs BC mass, colored by CO, both above (FT) and below (MBL) the inversion, **(b)** SO_4 vs BC mass, colored by CO, and **(c)** Org and **(d)** SO_4 vs BC Mass under 0.02 µg m^{-3} and CO less than 61 ppb.

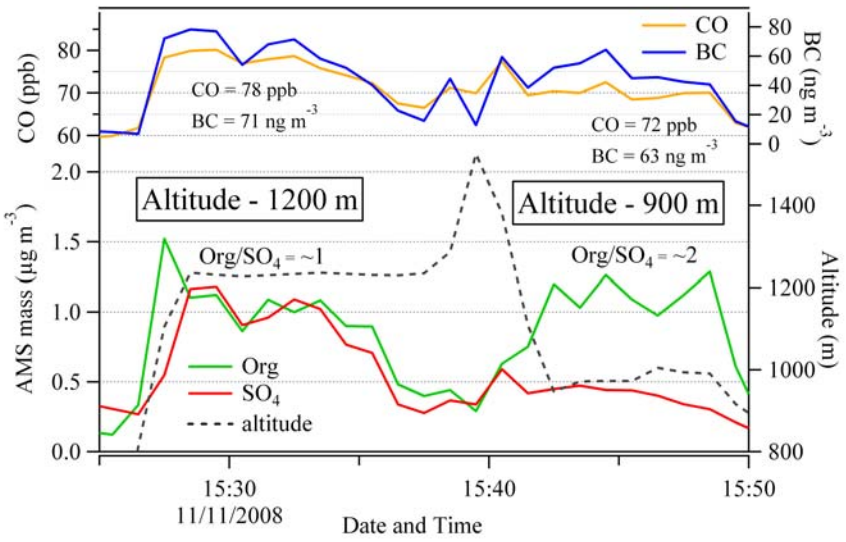

Figure 22. VOCALS FT pollution layers. Note the different concentrations of CO, SO_4, and BC in the two level legs which vary only 300 m in altitude.

level legs, with air masses 300 m different in altitude, which reveal different chemistry. The first level leg (between 15:28 and 15:38 UTC) is at 1200 m and shows an Org/SO_4 ratio of 1, with CO about 78 ppb and a BC mass concentration of 71 ng m^{-3}. Less than 10 minutes later, and at 900 m altitude (15:42 – 15:50 UTC), the Org/SO_4 ratio was 2, SO_4 having decreased from 1 ug m^{-3} to 0.5 ug m^{-3}, and though CO and BC were reduced to 72 ppb and 63 ng m^{-3}, respectively, the ratio CO/BC remained essentially constant (~1.1).

Figure 21c shows the strong relationship between Org and BC for BC values under 20 ng m^{-3} and CO < 61 ppb. The regression has an intercept of 0, and a R^2 value of 0.66, suggesting a significant linear relationship and a common anthropogenic source even for these low CO values. This is not true for the weak regression between SO_4 and BC over this same range (Fig. 20d). Also evident is a residual and variable SO_4 concentration when BC approaches our detection limit and CO is near the minimum of 50 ppb (dark blue). This is an expected result for clean background marine air, given SO_4

has a known and well-documented oceanic source (Andreae and Barnard, 1984; Andreae and Raemdonck, 1983; Cline and Bates, 1983).

However, we note a residual and variable SO_4 concentration when BC approaches our detection limit and CO is near the minimum of 50 ppb (dark blue circles). Below 1.8 ng m^{-3} BC there appears to be no relationship between SO_4 and BC (Fig. 21d). This SO_4 is likely to be of marine origin, so any correlation with Org may represent Org with a similar marine origin. Below 1.8 ng m^{-3} BC, and at a concentration of CO which highlights the low CO branch of the SO_4 versus BC relationship (determined to be 56 ppb), the natural marine variability in SO_4 is represented (Fig. 21d), i.e., SO_4 varies from 0.05-.5 μg m^{-3} (average 0.14 ± 0.11) while CO and BC remain essentially constant. Therefore, SO_4 and Org were further restricted to these values (CO < 56 ppb and BC < 1.8 ng m^{-3}) to more closely examine this low CO branch (dark blue circles in Fig. 21d) of the SO_4 vs Org relationship.

The relationship between SO_4 and Org for this data is shown in Fig. 23. These values of Org and SO_4, free of combustion influence, were then bin-averaged for every 0.05 increment of SO_4, and are superimposed on the one-minute data from Fig. 21 with 1 σ error bars. A linear fit to the bin-averaged data suggests a relationship between Org and SO_4, with a slope of 0.08, possibly indicative of an oceanic source for this Org. However, there is a fundamental issue in that we have no strong evidence that any of the Org in this region is marine. Figure 21c provides evidence that all Org in the SEP is anthropogenically derived, therefore the "natural" Org mass estimates here can be considered at most 0.08 of that of SO_4. This provides us with an estimate for a clean Org

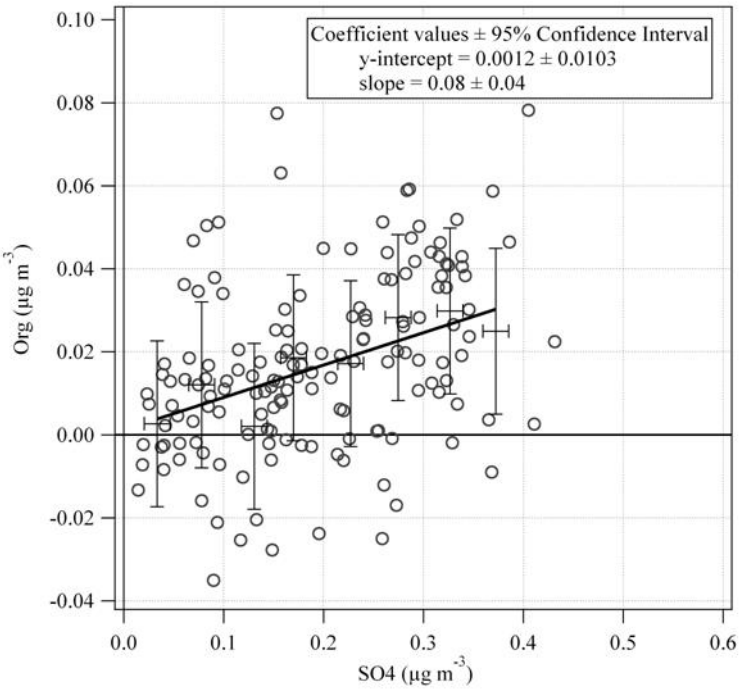

Figure 23. Natural Org vs. SO_4, one minute and bin-averaged data.

mass concentration for which to compare with other studies. It remains a possibility that no "clean" Org exists in this region.

Under these clean criteria, designed to isolate marine sulfate aerosol (CO < 56 ppb and BC mass < 1.8 ng m^{-3}) Org constitutes only 6% of total submicron, non-refractory aerosol mass, while SO_4 constitutes 87% of the total submicron non-refractory mass in the MBL. These results are somewhat below other studies in the tropics and subtropics and far smaller than those reported for high latitudes and phytoplankton blooms (Fig. 17) which find Org to make up 25-40% of the total submicron non-refractory mass, and even up to 77% in North Atlantic aerosols (O'Dowd and de Leeuw, 2007). Much of the difference is due to our use of very stringent BC criteria.

Approximate slopes of the Org/SO_4 ratio are drawn in Fig. 18, as visual representation of the relationships evident from various studies that all focused on clean marine aerosols: Trinidad Head (TH), Mace Head (MH), VOCALS Ron Brown (RB), Ace-Asia (AA), IMPEX (IMP) and Ocean Station Papa (OSP). The light blue triangle indicates the range of Org/SO_4 ratios from various biomass burning studies: the Western Arctic (McNaughton et al., 2011), Siberia and Kazakhstan (Warneke et al., 2009), and western Africa (Capes et al., 2008). We note that the average value for Mace Head (Org/SO_4 = 3.5) is plotted off scale but the implied slope falls within the ranges of Org/SO_4 ratios seen in these biomass burning studies. This indicates that at high latitudes the Org/SO_4 ratio is high, rivaling those found in biomass burning plumes.

4.2 Org enrichment during the TAO cruise

In order to explore the relation of the Org enhancement during the cruise (TAO* in Fig. 18) to possible ocean sources, eight-day composites of chlorophyll-*a* concentration were produced using SeaWIFS (Sea-viewing Wide Field-of-view- Sensor) Level 3 products provided by NASA/Goddard Space Flight Center (Ocean Color Web (http://oceancolor.gsfc.nasa.gov) accessed June 2010). Surface chlorophyll-*a* concentrations do not indicate a significant increase in biological production associated with aerosol measurements on the western boundary of the cruise track (Fig. 24a), compared to the eastern edge of the cruise (Fig. 24b, 11 September to 15 September). Maximum chlorophyll-*a* concentrations encountered within 3 days upwind of the ship track ranged from 0.2-0.3 mg m^{-3}, similar to concentrations found during periods of low biological activity in the O'Dowd et al., 2004 study. In contrast, during periods of high biological production activity, O'Dowd et al. reported a tenfold increase in chlorophyll-*a*

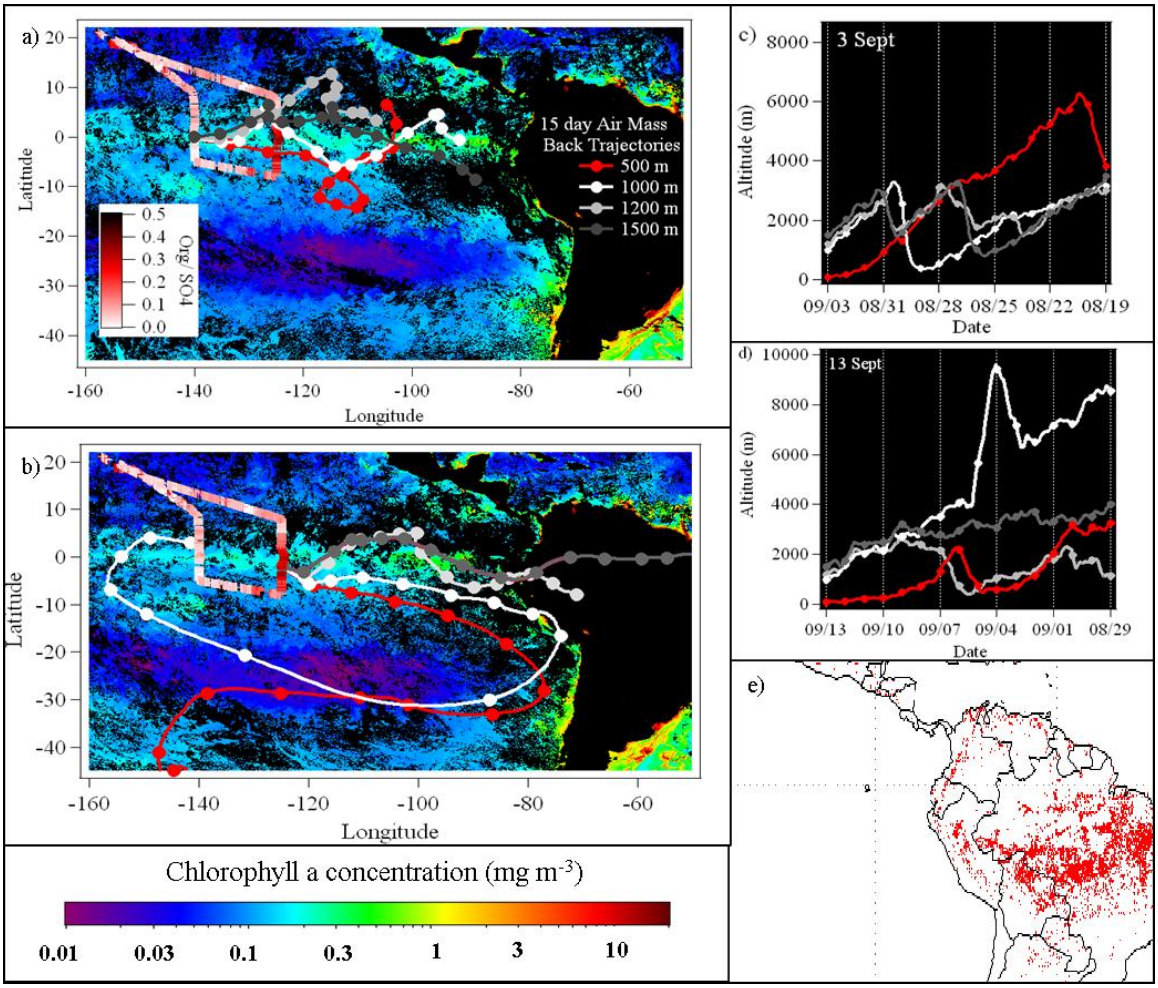

Figure 24. SeaWIFS chlorophyll-*a* 8 day composite for periods **(a)** 29 August–5 September 2009 overlaid by AMBTs from 3 September 2009 and **(b)** 6 September–13 September 2009 overlaid by AMBTs from 13 September 2009. Cruise track is shown, colored by Org/SO_4. AMBT altitude profiles are shown for **(c)** 3 September 2009 and **(d)** 13 September 2009. Altitude profiles are colored using the same legend as panel **a**. Panel **(e)** biomass burning events from 1 September – 8 September 2009 (FLAMBE').

concentrations that they associate with an enhancement of Org aerosol (from ~1 µg m^{-3} Org to ~5 µg m^{-3}).

Fifteen-day Air Mass Back Trajectories (AMBTs) were performed using the National Oceanic and Atmospheric Administration's (NOAA) Hybrid Single-Particle Lagrangian Integrated Trajectory (HYSPLIT) model access via NOAA ARL READY

website (http://www.arl.noaa.gov/ready/hysplit4.html). AMBTs are a tool used by atmospheric scientists to identify influences a particular air-mass has been in contact with. Isentropic trajectories were run at 4 altitudes (100 m, 1000 m, 1250 m, and 1500 m) using the GDAS meteorological dataset. The 100 m trajectory (red) origin was varied spatially by 1° north, south, east, and west, in order to capture spatial variability in the model. Within this spatial variation the trajectories were consistent for approximately the first 6 days of the AMBT, after which the 100 m trajectories tended to diverge. For simplicity, only one of the 100 m trajectories is displayed in Fig. 24. Several sets of trajectories were run, half during the peak of the Org/SO_4 excursion on the eastern most edge of the cruise track, and half on the western edge of the cruise track, where Org/SO_4 is close to the cruise-average 0.08 value. However, for clarity, only two sets of trajectories are plotted in Fig. 24. Altitude profiles for the AMBTs are shown in Fig. 24c and 24d.

AMBTs from one day, chosen to represent the western edge of the cruise track (3 September), indicate that influencing air masses have a) passed through the Inter-Tropical Convergence Zone (ITCZ), where convection and rainfall could have removed particulate matter, and b) spent the past 15 days over the ocean, with no indication of continental influence. The influence of ITCZ precipitation upon aerosol concentrations is clearly evident in Fig. 19 where they are reduced by up to a factor of four on 11 September and recover by 14 September. During this excursion the Org/SO_4 ratio shows little change, indicating no preferential removal of either species. This suggests the higher scavenging in the TAO region may have little impact on the ratio. AMBTs during the peak in the Org/SO_4 ratio from 13 September indicate that air masses have had possible continental influence in the past 15 days.

As previously noted for our VOCALS data, biomass burning in South America serves as a potential source of Org to the FT, and data from the Fire Locating and Modeling of Burning Emissions (FLAMBE' (http://www.nrlmry.navy.mil/flambe/) accessed July 2010) indicates widespread fires in the Amazon at the beginning of September, approximately 1-2 weeks before sampling occurred (Fig. 24e). Levoglucosan is a chemical tracer for biomass burning, as it is formed during the pyrolysis of cellulose (Simoneit et al., 1998). Lee et al. (2010) found that the AMS peak at m/z 60, more specifically $C_2H_4O_2$, a fragment resulting from the breakdown of levoglucosan and other anhydrosugars, including mannosan, galactosan, arabinosan, and xylosan, is an even better indication of biomass burning than levoglucosan itself. Using the high resolution data analysis and elemental analysis package for the AMS (Aiken et al., 2008), $C_2H_4O_2$ was identified and quantified by averaging the cruise data over ~12 h periods. Figure 25 shows the fraction of $C_2H_4O_2$ to total Org concentration, along with 12-h averaged Org/SO_4 overlaying the 10 min Org/SO_4 from Fig. 19. Because the signal to noise level is lower for the $C_2H_4O_2$ peak, error bars (1σ) are shown as well. The elevated $C_2H_4O_2$/Org between 11 September and 20 September drops at the transition from southern hemisphere air to northern hemisphere air (Fig. 19) suggesting that the increased Org can be associated with an increase in the relative amount of levoglucosan, indicating a biomass burning source in the southern hemisphere that is not present in the northern hemisphere. Levoglucosan was also detected at a ground-site in Paposo Chile during VOCALS, a region upwind of the TAO cruise area (Chand et al., 2010).

However, Russell et al. (2010) has determined that marine organics in the North Atlantic are primarily carbohydrate-like, and also show up at m/z 60 and 44. Although

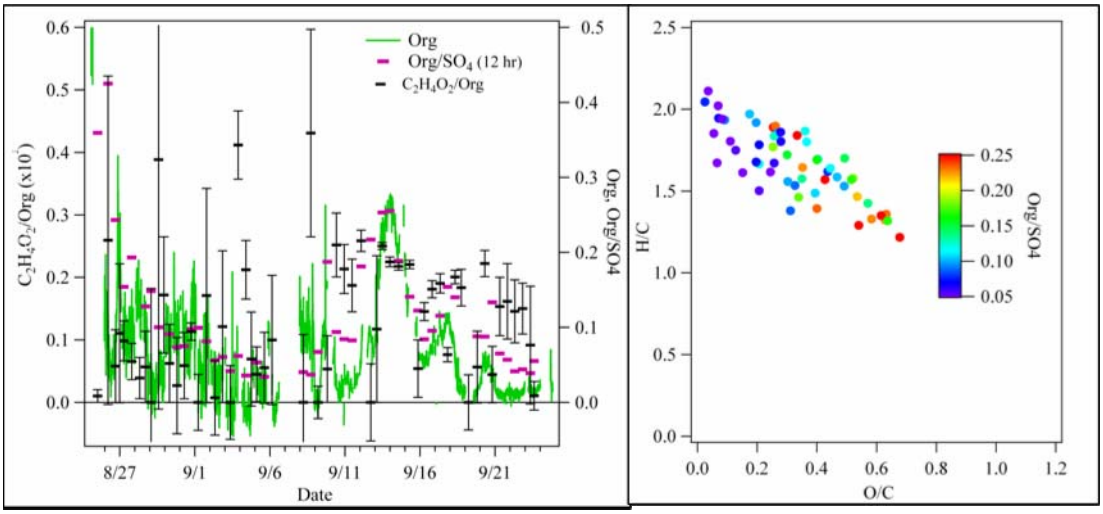

Figure 25. (Left) Time series of Org (10 min average), Org/SO_4 (12 h average), and $C_2H_4O_2$/Org (12 h). One sigma errors for the data are indicated. (Right) H/C vs O/C for the 12 h averaged data (Van Krevelen plot).

the fragment $C_2H_4O_2$ was not specifically mentioned in their study, we can't conclusively say the $C_2H_4O_2$ we measured is from biomass burning.

The 12 h averages of the elemental ratios H/C and O/C for this data are shown on a Van Krevelen plot (Heald et al., 2010) in Fig. 25 as well, and are colored by the Org/SO4 ratio. Heald et al. (2010) showed that a Van Krevelen diagram provides an indication of the amount of aging an aerosol has undergone, i.e., the longer an aerosol is in the atmosphere, the more oxidized it will become, and the H/C ratio will decrease while the O/C ratio will increase. Figure 25 reveals the more aged aerosol during TAO to be generally associated with the higher Org/SO_4 ratio, suggesting a non-local source for these aerosols. In contrast, values of Org/SO_4 near 0.08 are associated with a higher H/C, suggesting a more local, perhaps oceanic, source.

Although the AMBTs do not indicate a clear source of the rise in the Org/SO_4 ratio along the eastern edge of the TAO cruise track, SeaWIFS imagery does not suggest

the increased Org can be attributed to increased biological production. Transport in the FT appears reasonable as a potential source of Org to the Central Pacific MBL, similar to what was observed during VOCALS, but unfortunately no above-cloud data is available during the TAO cruise. However, such transport in the FT over this equatorial region has been noted in other papers (Hsu et al., 1996; Kim and Newchurch, 1996)

4.3 Potential instrument bias

Recent studies have determined that there is an under sampling of Org by the AMS, which could bias our results to lower values. For example, Hawkins et al. (2010) found the AMS had a particularly low CE in the VOCALS region during the same campaign (sampling in the MBL from the R/V *Ron Brown*). The low CE was associated with Org found on submicron dust particles originating from South America. However, dust particles are of continental origin, therefore low CE values associated with Org on dust would not impact the results of this study. Furthermore laboratory (Matthew et al., 2008) and field studies (Middlebrook et al., 2011) have shown CE for Org around 45% even with solid Org on crystalline sulfates. Primary marine Org appear to have been sampled well during a North Atlantic cruise (Russell et al., 2010), demonstrated by a 1:1 agreement between FTIR and AMS Org.

Another possible source of error that might bias the absolute values of Org low is through application of CE correction values to the data. A "worst case" scenario would be for a completely externally mixed aerosol, where Org are collected with about 50% efficiency and the SO_4 is not neutralized, and is therefore being collected with 100% efficiency. In this case, the CE scheme applied to our data would not account for the Org being under sampled (i.e., Org would not be properly multiplied by a correction factor of

2). However, a histogram of the CE values applied to the VOCALS campaign reveal that the CE lies between 0.5 and 0.7, 64% of the time (Fig. 26). Therefore, if anything, Org values for VOCALS are more likely to be overestimated by using the CE correction factors. A third possibility for under sampling of Org by our AMS could be the inlet efficiency. Calibrations have shown that there are significant particle losses by our AMS inlet at particle diameters greater than 600 nm, aerodynamic diameter. Hence, the potential for a significant Org fraction present on coarse sea-salt remains possible, although prior measurements of size resolved OM in marine aerosol find over 90% concentrated in sizes well resolved by our AMS (Fig. 14; O'Dowd et al., 2004). Plots and regression of Org vs. OPC coarse non-volatile mass (a sea-salt surrogate) – as used in the discussion of Fig. 15 also revealed no evidence of a relation between the OM concentrations measured by our AMS and sea-salt concentrations (Fig. 27). While this does not prove we are capturing coarse Org on sea-salt, it does not disprove it either.

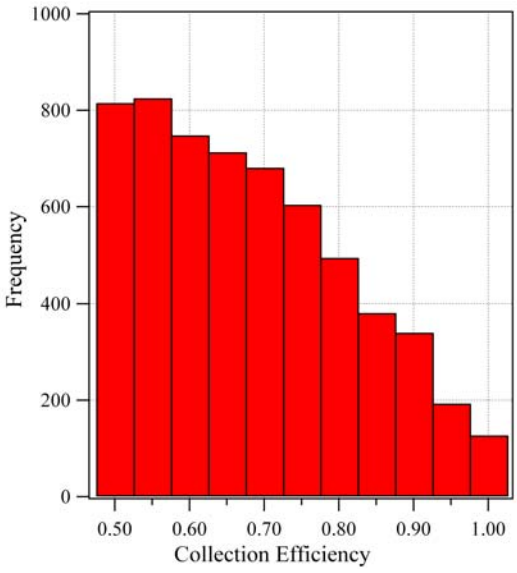

Figure 26. Histogram of the AMS CE during VOCALS.

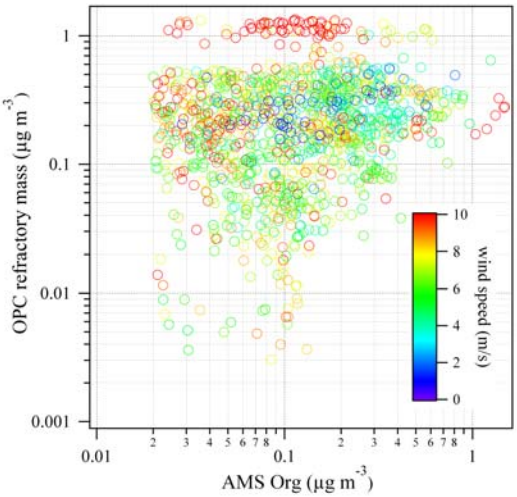

Figure 27. VOCALS MBL refractory OPC mass versus AMS Org mass.

There is also a significant distinction between primary and secondary organic aerosol, and what the AMS is able to sample. Recent studies have shown that much of the OM in marine aerosol is primary, emitted directly with sea-salt, rather than secondary, which forms from the oxidation of organic vapors. While sea-salt particles are typically too large for the AMS inlet, submicron particles are enriched in primary Org in the size range the AMS should measure (Keene et al., 2007). Our results are not consistent with studies such as Keene et al. (2007), which found a significant amount of primary submicron Org aerosol, even over oligotrophic ocean. Their experiment involved bubbling zero air through seawater, where they measured aerosol in the same size range as the AMS, and found Org concentrations roughly an order of magnitude (~0.1 µg m^{-3}) greater than observed during VOCALS and TAO.

4.4 Potential sampling bias

It is striking that at the same time and place, the Ron Brown found a much higher Org/SO_4 ratio. Unfortunately, incompatible instrumentation made it hard to do direct

comparisons. The C-130 lacked the radon (Rn) measurements used aboard the ship to detect continental influence and the ship lacked CO and SP2 measurements, so a common definition of clean air cannot be made. On the Ron Brown Rn was used to classify roughly 40% of the cruise as having Marine Air Mass (MAM) characteristics, but PMF analysis showed that something like 75% of the OM during those periods fit their combustion factor rather than the marine factor. Therefore, of their average MAM an OM of 0.4 $\mu g\ m^{-3}$, only about 0.1 $\mu g\ m^{-3}$ is of marine origin. It is not clear what fraction of the SO_4 is marine, so their Org/SO_4 ratio from marine sources is between 0.15 and 0.6. The lower end is still above our estimate of 0.1, but not by a large margin. Differences in the campaign Org/SO_4 ratios between the C-130 and Ron Brown are shown in Fig. 28a and b as histograms of the ratio. Ron Brown AMS Org were reported as 0 for concentrations below their instrument's detection limit (< 0.16 $\mu g\ m^{-3}$), biasing average concentrations low. In order to decrease this bias, for the purpose of this comparison, Org concentrations below instrument detection limits were replaced with half of that detection limit (0.08 $\mu g\ m^{-3}$). For the unrestricted cases, i.e., no clean air selection criteria applied, the Ron Brown observed higher Org/SO_4 ratios than the C-130. However, when CN is used as a clean air indicator, and is restricted to cases < 700 per cm^3 and < 350 per cm^3, the peak values of the frequency distributions of Org/SO_4 for the two platforms show better agreement. It should be noted that although CN is not a direct indicator of pollution as is the use of CO and BC, it was the only common measurement across the sampling platforms. This result suggests that during VOCALS, the Ron Brown was more frequently in contact with more continentally influenced air than the C-130, and therefore observed higher absolute and relative concentrations of Org during the

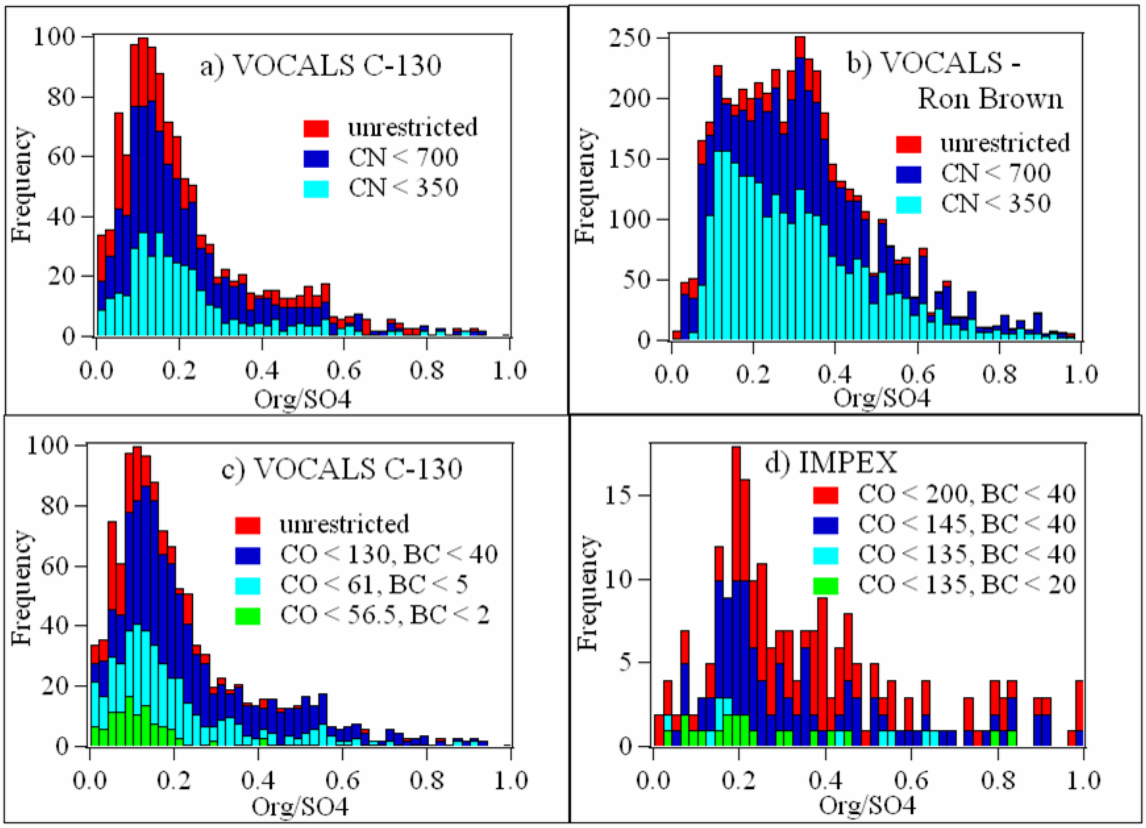

Figure 28. Histograms of Org/SO_4 from different platforms and campaigns, restricted to varying clean air criteria. Units are as follows: CN (cm^{-3}), CO (ppb), and BC (ng m^{-3}).

campaign. Figure 28c shows the Org/SO_4 histograms during VOCALS, but constrained to clean air cases using varying, and increasingly more restrictive, concentrations of BC and CO. These criteria yield narrower frequency distributions of Org/SO_4, and also shifted to lower Org/SO_4 values, than the more indirect index of pollution (CN). For both platforms the most frequent ratios under cleanest conditions are between about 0.1 and 0.2.

Histograms of Org/SO_4 ratios for IMPEX are shown in Fig. 28d. The Northern Hemisphere is generally more polluted, and therefore CO and BC concentrations were well above the low levels observed in the Southeast Pacific. In an effort to duplicate the

Mace Head clean air criteria, similar values of CO and BC were chosen to restrict the AMS data. The frequency distributions of the Org/SO_4 ratio are similar to those observed in VOCALS, and indicate an average Org/SO_4 ratio of about 0.16-0.20. Unfortunately, the clean IMPEX data suffers from poor statistics, the main objective of the campaign was to study the transport of pollution across the Pacific, and therefore few cases of clean air were encountered. The clean Org/SO_4 ratio that was observed during IMPEX is significantly lower than other studies in the North Pacific (i.e., Allan et al., 2004; Phinney et al., 2006). This is due to the rapid responses of the SP2 and CO allowing for the stricter stratification of data into clean and polluted cases. Alternatively, coastal studies such as Allan et al., maybe influenced by high productivity near the coast.

4.5 Potential method bias

Not all measurements of Org compared in this study are equal. Some studies (O'Dowd et al. 2004, Cavalli et al., 2004, Quinn and Bates 2003, Phinney et al., 2006) rely on filter-based measurements of OC. Filter measurements have significant biases, including negative artifacts from volatilization of particulate-phase organics from the filter surface, and positive artifacts from adsorption of gas-phase organics onto the filter (Turpin et al., 2000). Filter measurements do not, however, suffer from the potential refractory-Org losses as the AMS does. There is also the issue of particle bounce off the collection substrate of an impactor stage during sampling, leading to inaccurate size classifications. Also, in order to convert total organic carbon (TOC) from bulk filter measurements to water soluble and insoluble organic carbon (e.g. Cavelli et al., 2004) and total particulate organic matter (e.g. Quinn and Bates, 2003), TOC measurements from filters are multiplied by a conversion factor which represents a ratio between

molecular mass and carbon mass. These factors, when added to the AMS biases, can contribute to possible differences when comparing studies of OM measurements. It should be noted that for the purposes of this study the term Org, which is used in the AMS community to represent the amount of POM resolved by the AMS, is used interchangeably with POM from e.g. Quinn and Bates, 2003 and WIOC+WSOC (e.g. from Cavelli et al., 2004).

The same issue is true for the different methods of measuring black carbon. Filter-based techniques for measuring black carbon, such as with instruments as the aethelometer (as used in Cavelli et al., 2004), and the particle soot absorption photometer (PSAP), use a difference in the transmission of light through a filter as it becomes loaded with aerosol. This measure of aerosol light absorption is then related to total BC through empirical formulas (Lack et al., 2008). Errors to filter-based instruments include deposit and filter matrix interactions which may change the physical and optical properties of the system, leading to inaccurate light absorption measurements, as well as the use of empirical corrections which can alter the measured change in transmission, limiting accuracies to between 20–30% (Bond et al., 1999; Virukula et al., 2005; Weingartner et al., 2003).

4.6 Implications for modeling studies

Modeling sea-spray aerosol, and the organic aerosol contribution to the global emission, has been the subject of recent studies (Langmann et al., 2008, O'Dowd et al., 2008, Vignati et al., 2010). Several relationships have been used to relate water insoluble organic mass fraction to surface chlorophyll-*a* concentrations upwind of the measurements. Some data used to establish these relationships can be found in O'Dowd

et al. (2008), and are duplicated in Fig. 29. Modeling studies that employ these functions to extrapolate OA production globally often overestimate Org aerosol concentrations by a factor of 4 or 5 compared to observations (Lapina et al., 2011, Westervelt et al., 2011). However, the VOCALS, TAO, and IMPEX Org contributions to total submicron mass (6%, 7%, 18%, respectively) and monthly averaged chlorophyll-*a* concentrations (from SeaWIFS) in surface water upwind of these study areas, yield data points that lie well below the linear function found in O'Dowd et al. (2008), Langmann et al. (2008), and Vignati et al. (2010), and are also plotted in Fig. 29. However, our data are within the low percent Org mass (0-20%), low chlorophyll-a (0.15-0.2 mg m^{-3}) regime of the O'Dowd (2008) data, suggesting a relationship that goes through the origin rather than

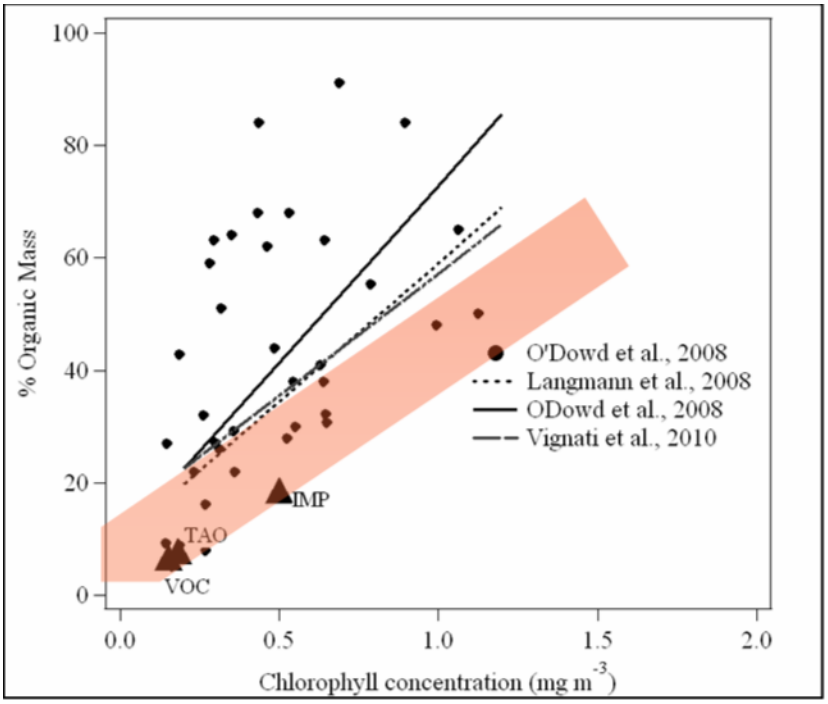

Figure 29. Organic-inorganic sea-spray source functions from recent studies (adapted from O'Dowd et al., 2008, Langmann et al., 2008, Vignati et al., 2008). Campaign averaged data from VOCALS, TAO, IMP are indicated by triangles. The red shading illustrates that a range of values of Chlorophyll-*a* and % Organic Mass is a more likely representation of this relationship.

having a significant intercept at zero chlorophyll-*a*. This would suggest the higher ratios for Mace Head may reflect non-oceanic source of Org or uncertainties in effective chlorophyll-*a*. If a relationship that encompasses our data were used for models then the modeled Org mass for the mean global chlorophyll of 0.36 mg m^{-3} (Siegel et al., 2002) should drop from values near 30% to values near 15%, or about a factor of two.

5 Conclusion

Our measurements in air over the remote South Pacific during VOCALS revealed low Org concentration in marine aerosol with values that trended linearly with combustion derived BC mass concentrations down to values of BC < 2 ng m^{-3}. This was made possible by the relatively rapid measurements of Org and BC made possible by an HR-ToF-AMS and an SP2. This raises questions about the appropriate choice of a clean threshold for BC used to eliminate influences of combustion aerosol when characterizing background marine aerosol. In fact, the concept of establishing background conditions is insufficient and it is necessary to either demonstrate that the natural aerosols overwhelm the anthropogenic influences such that they can be ignored, or employ some technique to isolate marine from continental aerosols, such as the use of carbon isotopes (e.g., Ceburnis et al., 2011). During VOCALS, the linear relationship between BC mass and Org suggests that most, if not all, Org in this region is associated with biomass burning and pollution, and that the ocean in this remote region is not a major source of Org to the marine atmosphere.

Relative concentrations of clean SO_4 and Org during the TAO 2009 cruise and VOCALS campaign reveal that only a small percentage of submicron non-refractory

aerosol mass is Org (~6 % for VOCALS, ~7 % for TAO). While the low values we found of Org/SO_4 due to marine sources is smaller than many studies from tropical and subtropical regions, those studies generally characterized the air during relatively clean periods; isolating marine from continental fractions was not feasible. Therefore, our conclusion that OA is not a major fraction of clean marine aerosol is not inconsistent. While highly productive regions of the ocean are well documented as a major source of OA, Org appears to have a much smaller role over the vast, relatively unproductive majority of the oceans. The findings from IMPEX were similar to VOCALS and TAO, where the mode Org/SO_4 ratios decreased to smaller and smaller values as clean air criteria were restricted to lower BC and CO concentrations.

Although our results are for regions of lower productivity than some of these investigations, a recent study by Claeys et al. (2010) found Org mass contributes less than 10% to total submicron mass in aerosols collected at Amsterdam Island, with similar Org mass concentrations as seen during VOCALS and TAO. This was true even during periods of high biological production, demonstrating results that are in agreement with observations from this study.

Comparison of the percent of Org in the aerosol and satellite-derived chlorophyll-*a* concentrations for VOCALS, TAO, and IMPEX yielded a relationship that goes through the origin and with a slope similar to others reported in the literature for this relationship (Langmann et al., 2008; O'Dowd et al., 2008; Vignati et al., 2010) but their non-zero intercept at zero chlorophyll-*a* concentrations does not reflect the lower values we find here for low chlorophyll-*a* regions. This would reduce associated estimates of the contribution of marine Org in the aerosol by a factor of two or so for the lower

chlorophyll concentrations representative of the typical global ocean. If employed in models, this could improve consistency between measurements and model observations, particularly over less productive regions of the oceans.

We believe the lower values of marine Org from our studies can be attributed, at least in part, to collection taking place 1) in the Southern Hemisphere, where there is less population and landmass, 2) over a remote area of the ocean typically far removed from continental influence, and 3) over relatively unproductive ocean regions, therefore less primary and secondary organic aerosol. Hence, chemical pollution indicators, such as CO and BC, are at significantly lower concentrations in the Southeast Pacific, providing lower thresholds with which to stratify data into clean and polluted cases and test for trends. Org and BC trended linearly (R^2=0.66, y-intercept of 0), suggesting that Org in VOCALS region is anthropogenically derived, and that the ocean surface is not a significant source of submicron, non-refractory Org. Much of the VOCALS SO_4 concentrations also varied with BC, reflecting a combustion influence. However, others did not and revealed variability in SO_4 between about 0.05 and 0.5 $\mu g\ m^{-3}$ when BC was at our detection limit of about 2 $ng\ m^{-3}$. At these low values of BC and CO, average SO_4 values were $0.14 \pm 0.11\ \mu g\ m^{-3}$ and Org concentrations were $0.01 \pm 0.02\ \mu g\ m^{-3}$. Although BC measurements were not taken during TAO 2009, plots of Org vs SO_4 suggest background conditions similar to those found in the MBL during VOCALS. Although we focus here on marine MBL aerosol, our data in the FT for VOCALS revealed elevated combustion aerosol aloft suggesting it must be considered as a potential source of Org to the MBL in remote regions.

Acknowledgements

I would like to thank the crews of the NCAR C-130 and NOAA R/V *Ka'imimoana* for their assistance in collecting this data. This work is funded under ONR grant #N000014-07-0031 and NSF grant #ATM07-45368. I would also like to acknowledge P. DeCarlo, J. Jimenez, G. Kok, and E. Dunlea for the use of the IMPEX data, as well as P. Quinn and T. Bates for the VOCALS Ron Brown data (available at http://saga.pmel.noaa.gov/data). I would like to thank my chairperson and advisor, Antony Clarke, and my committee members Barry Huebert and Steven Howell for their input, guidance, and support.

Appendix A. SQUIRREL fragmentation table adjustments

Adjustments to the fragmentation table during SQUIRREL processing were mostly achieved by altering the air mass fragment coefficient at m/z 29 (frag_air[29]), see Table A1. The default coefficient is used to represent an isotopic factor and describes the relative amount of $N^{15}N$ at m/z 29, which is related to the signal of N_2 at m/z 28. The N_2 peak is usually the largest, or sometimes second largest, peak. It has poor shape and baseline distortions that yield small, but constant, errors in the integration of this peak. This is to be expected, however, because of these effects, coupled with threshold setting and possible saturation effects, the isotopic factor used to calculate the $N^{15}N$ peak may be slightly different than predicted. Therefore it may be multiplied by a factor, close to 1, in order to correct the negative Org signal at m/z 29 during a filter period (see Table 2). Table 2 shows an example of the fragmentation table used in SQUIRREL, with common changes indicated in bold. Most table adjustments have to do with the potential saturation of the N_2 peak at m/z 28, for the reasons mentioned above.

Table A1. Example fragmentation table for SQUIRREL processing. Common adjustments are highlighted in bold.

m/z	frag_air	frag_CO2	frag_water	frag_RH	frag_organic
14	14,-frag_nitrate[14]				
15	0.00368* frag_air[14]				15,-frag_NH4[15], -frag_air[15]
16	frag_O16[16], frag_RH[16]		0.04* frag_water[18]	0.04* frag_RH[18]	0.04* frag_organic[18]
17	0.000391* frag_O16[16], frag_RH[17]		0.25* frag_water[18]	0.25* frag_RH[18]	0.25* frag_organic[18]
18	0.002* frag_O16[16], frag_RH[18]		18,-frag_air[18], -frag_sulph [18],-frag_org [18]	**0.01* frag_air[28]**	0.225* frag_organic[44]
19	frag_RH[19]		0.000691* frag_water[18],0.002* frag_water[17]	0.000691* frag_RH[18], 0.002* frag_RH[17]	0.000691* frag_organic[18], 0.002* frag_organic[17]
20	20,-frag_org [20], -frag_sulph [20],-frag_water[20]		0.002* frag_water[18]	0.002* frag_RH[18]	0.002* frag_organic[18]
24					24,-frag_sulph[24]
28	28				frag_organic[44]
29	**(0.00736 *0.87)* frag_air[28]**				29,-frag_air[29]
30	0.0000136* frag_air[28]				0.022* frag_organic[29]
31					31,-frag_nitrate[31]
32	32,-frag_ sulphate[32],-frag_nitrate[32]				
33	0.000763* frag_air[32]				
34	0.00402* frag_air[32]				
36	0.00338* frag_air[40]				
37					37,-frag_chl[37]
38	0.000633* frag_air[40]				38,- frag_chl [38],-frag_air[38]
40	0.009*1.11* 1.28* 1.14* frag_air[28]				
41					41,-frag_K[41]
44	frag_CO2[44]	**0.00037*1.36 *1.28*1.14* frag_air[28]**			44,-frag_air[44]

References

Aiken, A.C., DeCarlo, P.F., Kroll, J.H., Worsnop, D.R., Huffman, J.A., Docherty, K.S., Ulbrich, I.M., Mohr, C., Kimmel, J.R., Sueper, D., Sun, Y., Zhang, Q., Trimborn, A., Northway, M., Ziemann, P.J., Canagaratna, M.R., Onasch, T.B., Alfarra, M.R., Prevot, A.S.H., Dommen, J., Duplissy, J., Metzger, A., Baltensperger, U., and Jimenez, J.L.: O/C and OM/OC ratios of primary, secondary, and ambient organic aerosols with High-Resolution Time-of-Flight Aerosol Mass Spectrometry, Environ. Sci. Technol., 42, 4478–4485, 2008.

Ackerman, A.S., Toon, O.B., Taylor, J.P., Johnson, D.W., Hobbs, P.V., and Ferek, R.J.: Effects of Aerosols on Cloud Albedo: Evaluation of Twomey's Parameterization of Cloud Susceptibility Using Measurements of Ship Tracks. J. Atmos. Sci., 57, 2684–2695, 2000.

Albrecht, B. A.: Aerosols, cloud microphysics, and fractional cloudiness, Science, 245, 1227–1230, 1989.

Allan, J.D., Bower, K.N., Coe, H., Boudries, H., Jayne, J.T., Canagaratna, M.R., Millet, D.B., Goldstein, A.H., Quinn, P. K., Weber, R.J., and Worsnop, D.R.: Submicron aerosol composition at Trinidad Head, California, during ITCT 2K2: Its relationship with gas phase volatile organic carbon and assessment of instrument performance, J. Geophys. Res., 109, D23S24, doi:10.1029/2003JD004208, 2004.

Allen, G., Coe, H., Clarke, A., Bretherton, C., Wood, R., Abel, S. J., Barrett, P., Brown, P., George, R., Freitag, S., McNaughton, C., Howell, S., Shank, L., Kapustin, V., Brekhovskikh, V., Kleinman, L., Lee, Y.-N., Springston, S., Toniazzo, T., Krejci, R., Fochesatto, J., Shaw, G., Krecl, P., Brooks, B., McKeeking, G., Bower, K. N., Williams, P. I., Crosier, J., Crawford, I., Connolly, P., Covert, D., and Bandy, A. R.: Southeast Pacific atmospheric composition and variability sampled along 20° S during VOCALS-REx, Atmos. Chem. Phys., 11, 5237-5262, doi:10.5194/acp-11-5237-2011, 2011.

Andreae, M.O. and Barnard, W.R.: The marine chemistry of dimethylsulfide, Mar. Chem., 14, 267-279, 1984.

Andreae, M. O., Elbert, W., Cai, Y., Andreae, T. W., and Gras, J.: Non-sea-salt sulfate, methanesulfonate, and nitrate aerosol concentrations and size distributions at Cape Grim, Tasmania, J. Geophys. Res., 104, 21695-21706, 1999.

Andreae, M.O. and Raemdonek, H.: Dimethyl sulfide in the surface ocean and the marine atmosophere: a global view, Science, 221, 744-747, 1983.

Baker, M.B. and Charlson, R.J.: Bistability of CCN concentrations and thermodynamics in the cloud-topped boundary layer, Nature, 245, 142-145, 1990.

Baron, P.A. and Willeke, K. (editors): Aerosol Measurement: Principles, Techniques and Applications (second edition), 1144 pp., John Wiley & Sons, Hoboken, New Jersey, 2001.

Bates, T., Quinn, P., Coffman, D., Johnson, J., and Middlebrook, A.: Dominance of organic aerosols in the marine boundary layer over the Gulf of Maine during NEAQS 2002 and their role in aerosol light scattering, J. Geophys. Res., 110, 2005.

Bodhaine, B.A., Deluisi, J.J., Harris, J.M., Houmere, P., and Bauman, S.: Aerosol measurements at the South Pole, Tellus B, 38B, 223-235, 1986.

Bond, T. C., Anderson, T. L. and Campbell, D.: Calibration and Intercomparison of Filter-Based Measurements of Visible Light Absorption by Aerosols, Aerosol Sci. Technol., 30, 582, 1999.

Bretherton, C.S., Wood, R., George, R.C., Leon, D., Allen, G., and Zheng, X.: Southeast Pacific stratocumulus clouds, precipitation and boundary layer structure sampled along 20S during VOCALS-Rex, Atmos. Chem. Phys., 10, 10639-10654, doi:10.5194/acp-10-10639-2010, 2010.

Canagaratna, M. R., Jayne, J. T., Jimenez, J. L., Allan, J. D., Alfarra, M. R., Zhang, Q., Onasch, T. B., Drewnick, F., Coe, H., Middlebrook, A., Delia, A., Williams, L. R., Trimborn, A. M., Northway, M. J., DeCarlo, P. F., Kolb, C. E., Davidovits, P., and Worsnop, D. R.: Chemical and microphysical characterization of ambient aerosols with the Aerodyne aerosol mass spectrometer, Mass Spectrom. Rev., 26, 185-222, doi:10.1002/mas.20115, 2007.

Cavalli, F., Facchini, M.C., Decesari, S., Mircea, M., Emblico, L., Fuzzi, S., Ceburnis, D., Yoon, Y.J., O'Dowd, C.D., Putaud, J.-P., and Dell'Acqua, A.: Advances in characterization of size-resolved organic matter in marine aerosol over the North Atlantic, J. Geophys. Res., 109, D24215, doi:10.1029/2004JD005137, 2004.

Ceburnis D., Garbaras, A., Szidat, S., Rinaldi, M., Fahrni, S., Perron, N., Wacker, L., Leinert, S., Remeikis, V., Facchini, M.C., Prevot, A.S.H., Jennings, S. G., Ramonet, M., and O'Dowd, C.D.: Quantification of the carbonaceous matter origin in submicron marine aerosol by ^{13}C and ^{14}C isotope analysis, Atmos. Chem. Phys., 11, 8593–8606, 2011.

Chand, D., Hegg, D.A., Wood, R., Shaw, G.E., Wallace, D., and Covert, D.S.: Source attribution of climatically important aerosol properties measured at Paposo (Chile) during VOCALS., Atmos. Chem. Phys., 10, 10789-10801, doi:10.5194/acp-10-10789-2010, 2010.

Charlson, R. J., Lovelock, J.E., Andreae, M.O., and Warren, S.G.: Oceanic phytoplankton, atmospheric sulfur, cloud albedo and climate, Nature, 326, 655-661, 1987.

Clarke, A.D., A thermo-optic technique for *in situ* analysis of size-resolved aerosol physiochemistry, Atmos. Environ., 25A, 635-644, 1991.

Clarke, A.D., Collins, W.G., Rasch, P.J., Kapustin, V.N., Moore, K., Howell, S., and Fuelberg, H.E.: Dust and pollution transport on global scales: Aerosol measurements and model predictions, J. Geophys. Res., 106, 32555-32569, 2001.

Clarke, A.D. and Kapustin, V.N.: Hemispheric aerosol vertical profiles: Anthropogenic impacts on optical depth and cloud nuclei, Science, 329, 1488-1492, 2010.

Clarke, A.D., Varner, J.L., Eisele, F., Tanner, R., Mauldin, L., and Litchy, M.: Particle production in the remote marine atmosophere: Cloud outflow and subsidence during ACE-1, J. Geophys, Res., 103, 16397-16409, 1998.

Claeys, M., Wang, W., Vermeylen, R., Kourtchev, I., Chi, X., Farhat, Y., Surratt, J.D., Gómez-González, Y., Sciare, J., and Maenhaut, W.: Chemical characterization of marine aerosol at Amsterdam Island during the austral summer of 2006-2007, J. Aerosol Sci., 41, 13-22, 2010.

Cline, J.D., and Bates, T.S.: Dimethyl sulfide in the Equatorial Pacific: A natural source of sulfur to the atmosphere, Geophys. Res. Lett., 10, 949-952, 1983.

Cross, E. S., Slowik, J. G., Davidovits, P., Allan, J. D., Worsnop, D. R., Jayne, J. T., Lewis, D. K., Canagaratna, M., and Onasch, T. B.: Laboratory and ambient particle density determinations using light scattering in conjunction with aerosol mass spectrometry, Aerosol Sci. Technol., 41, 343-359, 2007.

Dall'Osto, M., Ceburnis, D., Martucci, G., Bialek, J., Dupuy, R., Jennings, S.G., Berresheim, H., Wenger, J., Healy, R., Facchini, M.C., Rinaldi, M., Giulianelli, L., Finessi, E., Worsnop, D., Ehn, M., Mikkilä, J., Kulmala, M., and O'Dowd, C. D.: Aerosol properties associated with air masses arriving into the North East Atlantic during the 2008 Mace Head EUCAARI intensive observing period: an overview, Atmos. Chem. Phys., 10, 8413-8435, 2010.

DeCarlo, P.F., Kimmel, J.R., Trimborn, A., Northway, M.J., Jayne, J.T., Aiken, A.C., Gonin, M., Fuhrer, K., Horvath, T., Docherty, K.S., Worsnop, D.R., and Jimenez, J.L.: Field-deployable, High-Resolution, Time-of-flight Aerosol Mass Spectrometer, Anal. Chem., 78, 8281-8289, 2006.

Drewnick, F., Schwab, J.J., Hogrefe, O., Peters, S., Husain, L., Diamond, D., Weber, R., Demerjian, K.L.: Intercomparison and evaluation of four semi-continuous PM-2.5 sulfate instruments. Atmos. Environ., 37, 3335–3350, 2003.

Dunlea, E. J., DeCarlo, P.F., Aiken, A.C., Kimmel, J.R., Peltier, R. E., Weber, R. J., Tomlinson, J., Collins, D.R., Shinozuka, Y., McNaughton, C.S., Howell, S.G., Clarke, A.D., Emmons, L.K., Apel, E.C., Pfister, G.G., van Donkelaar, A., Martin, R.V., Millet,

D.B., Heald, C.L., and Jimenez, J.L.: Evolution of Asian aerosols during transpacific transport in INTEX-B, Atmos. Chem. Phys., 9, 7257-7677, 2009.

Gerbig, C., Schmitgen, S., Kley, D., Volz-Thomas, A., Dewey, K.,and Haaks, D.: An improved fast-response vacuum-UV resonance fluorescence CO instrument, J. Geophys. Res., 104, 1699–1704, 1999.

Grenfell, J.L.: An analysis of rapid increases in condensation nuclei concentrations at a remote coastal site in Western Ireland, J. Geophys. Res., 104, 13771-13780, 1999.

Gysel, M., Laborde, M., Olfert, J.S., Subramanian, R., and Grohn, A. J.: Effective density of Aquadag and fullerene soot black carbon reference materials used for SP2 calibration, Atmos. Meas. Tech. Discuss., 4, 4937-4955, 2011.

Haywood, J.M., Osborne, S.R., Francis, P.N., Keil,A., Formenti, P., Andreae, M.O., and Kaye, P.H.: The mean physical and optical properties of regional haze dominated by biomass burning aerosol measured from the C-130 aircraft during SAFARI 2000, J. Geophys. Res., 108, 2003.

Hawkins, L.N., Russell, L.M., Covert, D.S., Quinn, P.K., and Bates, T.S.: Carboxylic acids, sulfates, and organosulfates in processed continental organic aerosol over the southeast Pacific Ocean during VOCALS-Rex 2008, J. Geophys. Res., 115, D13201, doi:10.1029/2009JD013276, 2010.

Heald, C.L., Kroll, J.H., Jimenez, J.L., Docherty, K.S., DeCarlo, P.F., Aiken, A.C., Chen, Q., Martin, S.T., Farmer, D.K., and Artaxo, P.A.: A simplified description of the evolution of organic aerosol composition in the atmosphere, Geophys. Res. Lett., 37, L08803, doi:10.1029/2010GL042737, 2010.

Hsu, N.C., Herman, J.R., Bhartia, P.K., Seftor, C.J., Torres, O., Thompson, A.M., Gleason, J.F., Eck, T.F., and Holben, B.N.: Detection of biomass burning smoke from TOMS measurements, Geophys. Res. Lett., 23, 745-748, 1996.

Hoffman, E.J. and Duce, R.A.: The organic carbon content of marine aerosol collected on Bermuda, J. Geophys. Res., 79, 4474-4477, 1976.

Huffman, J. A., Jayne, J.T., Drewnick, F., Aiken, A.C., Onash, T., Worsnop, D.R., and Jimenez, J.L.: Design, modeling, optimization, and experimental tests of a particle beam width probe for the Aerodyne aerosol mass spectrometer, Aerosol Sci. Technol, 39, 1143-1163, doi:10.1080/02786820500423782, 2005.

IPCC: Climate Change 2007: The Physical Science Basis, in: Contribution of Working Group I to the Fourth Assessment Report of the Intergovernmental Panel on Climate Change, edited by: Solomon, S., Qin, D., Manning, M., Chen, Z., Marquis, M., Averyt, K.

B., Tignor, M., and Miller, H. L., Cambridge University Press, Cambridge, United Kingdom and New York, NY, USA, 996 pp., 2007.

Jacob, D. J.: Introduction to Atmospheric Chemistry, 1st ed., Princeton University Press, Princeton, New Jersey, 266 pp., 1999.

Jaffe, D., Anderson, T., Covert, D., Kotchenruther, R., Trost, B., Danielson, J., Simpson, W., Berntsen, T., Karlsdottir, S., Blake, D., Harris, J., Carmichael, G., and Uno, I.: Transport of Asian air pollution to North America, Geophys. Res. Lett., 26, 711-714, 1999.

Jaffe, D., Mahura, A., Kelley, J., Atkins, J., Novelli, P.C., and Merrill, J.: Impact of Asian emissions on the remote North Pacific atmosphere: Interpretation of CO data from Shemya, Guam, Midway, and Mauna Loa, J. Geophys. Res., 102, 28627-28635, 1997.

Jimenez, J.L.: Field Data Analysis Guide, online available: http://cires.colorado.edu/jimenez-group/wiki/index.php/Field_Data_Analysis_Guide, 2010.

Keene, W.C., Maring, H., Maben, J.R., Kieber, D.J., Pszenny, A.A.P., Dahl, E.E., Izaguirre, M.A., Davis, A.J., Long, M.S., Zhou, X., Smoydzin, L., Sander, R.: Chemical and physical characteristics of nascent aerosols produced by bursting bubbles at a model air-sea interface, J. Geophys. Res., 112, D21202, 2007.

Kim, J.H., and Newchurch, M.J.: Climatology and trends of tropospheric ozone over the eastern Pacific Ocean: The influences of biomass burning and tropospheric dynamics, Geophys. Res. Lett., 23, 3723-3726, 1996.

Kleefeld, S., Hoffer, A., Krivacsy, Z., and Jennings, S.G.: Importance of organic and black carbon in atmospheric aerosols at Mace Head, on the West Coast of Ireland, Atmos. Environ., 36, 4479-4490, 2002.

Lack , D. A. , Cappa , C. D. , Baynard , T. , Massoli , P. , Covert , D. S. , Sierau , B. , Bates , T. S. , Quinn , P. K. , Lovejoy , E. R. and Ravishankara , A. R.: Bias in Filter-Based Aerosol Absorption Measurements Due to Organic Aerosol Loading: Evidence from Ambient Measurements, Aerosol Sci. Technol., 42, 1033 – 1041, 2008.

Langmann, B., Varghese, S., Marmer, E., Vignati, E., Wilson J., Stier, P., O'Dowd, C.: Aerosol distribution over Europe: a model evaluation study with detailed aerosol microphysics, Atmos. Chem. Phys., 8, 1591-1607, 2008.

Lapina, K., Heald, C.L., Spracklen, D.V., Arnold, S.R., Allan, J.D., Coe, H., McFiggans, G., Zorn, S.R., Drewnick, F., Bates T.S., Hawkins, L.N., Russell, L.M., Smirnov, A., O'Dowd, C.D., Hind, A.J.: Investigating organic aerosol loading in the remote marine environment, Atmos. Chem. Phys. Discuss., 11, 10973-11006, doi:10.5194/acpd-11-10973-2011, 2011.

Lee, T., Sullivan, A.P., Mack, L., Jimenez, J.L., Kreidenweis, S.M., Onasch, T.B., Worsnop, D.R., Malm, W., Wold, C.E., Hao, W.M., Collet Jr., J. L.: Chemical smoke marker emissions during flaming and smoldering phases of laboratory open burning of wildland fuels, Aerosol Sci. Technol., 44, i-v, 2010.

Lohmann, U. and Leck, C.: Importance of submicron surface-active organic aerosols for pristine Arctic clouds, Tellus, 57B, 261-268, 2005.

Maßling, A., Wiedensohler, A., Busch, B., Neusüß, C., Quinn, P., Bates, T., and Covert, D.: Hygroscopic properties of different aerosol types over the Atlantic and Indian Oceans, Atmos.Chem. and Phys., 3. 1377–1397, doi:10.5194/acp-3-1377-2003, 2003.
Matthew, B.M., Middlebrook, A.M., and Onasch, T.B.: Collection efficiencies in an Aerodyne Aerosol Mass Spectrometer as a function of particle phase for laboratory generated aerosols, Aerosol Sci.. Technol., 42, 884-898, 2008.

McNaughton, C. S., Clarke, A. D., Freitag, S., Kapustin, V. N., Kondo, Y., Moteki, N., Sahu, L., Takegawa, N., Schwarz, J. P., Spackman, J. R., Watts, L., Diskin, G., Podolske, J., Holloway, J. S., Wisthaler, A., Mikoviny, T., de Gouw, J., Warneke, C., Jimenez, J., Cubison, M., Howell, S. G., Middlebrook, A., Bahreini, R., Anderson, B. E., Winstead, E., Thornhill, K. L., Lack, D., Cozic, J., and Brock, C. A.: Absorbing aerosol in the troposphere of the Western Arctic during the 2008 ARCTAS/ARCPAC airborne field campaigns, Atmos. Chem. Phys., 11, 7561-7582, 2011.

McNaughton, C.S., Clarke, A.D., Howell, S.G., Pinkerton, M., Anderson, B., Thornhill, L., Hudgins, C., Winstead, E., Diff, J.E., Scheuer, E., and Maring, H.: Results from the DC-8 inlet characterization experiment (DICE): Airborne versus surface sampling of mineral dust and sea salt aerosols, Aerosol Sci. Tech., 41, 136-159, 2007.

Middlebrook, A.M., Murphy, D.M., and Thomson, D.: Observation of organic material in individual marine particles at Cape Grim during the First Aerosol Characterization Experiment (ACE-1), J. Geophys. Res., 103, 16475-16483, 1998.

Middlebrook, A.M., Bahreini, R., Jimenez, J.L., and Canagaratna, M.R.: Evaluation of Composition-Dependent Collection Efficiencies for the Aerodyne Aerosol Mass Spectrometer using Field Data, Aerosol Sci. Tech., DOI:10.1080/02786826.2011.620041, 2011.

Miyazaki, Y., Kawamura, K., and Sawano, M.: Size distributions of organic nitrogen and carbon in remote marine aerosols: Evidence of marine biological origin based on their isotopic ratios. Geophys.Res. Lett., 37, L06803, 2010.

Moore, K.G. II., Clarke, A.D., Kapustin, V.N., McNaughton, C., Anderson, B.E., Winstead, E.L., Weber, R., Ma, Y., Lee, Y.N., Talbot, R., Dibb, J., Andersen, T., Doherty, S., Covert, D., and Rogers, D.:A comparison of similar aerosol measurements made on the NASA P3-B, DC-8, and NSF C-130 aircraft during TRACE-P and ACE-Asia, J. Geophys. Res., 109, D15S15, doi:10.1029/2003JD003543, 2004.

Moteki, N., and Kondo, Y.: Dependence of Laser-Induced Incandescence on Physical Properties of Black Carbon Aerosols: Measurements and Theoretical Interpretation, Aerosol Sci. Tech., 44, 663-675, 2010.

Narukawa, M., Kawamura, K., Li, S., and Bottenheim, J.: Stable carbon isotopic ratios and ionic composition of the high-Arctic aerosols: An increase in ∂13C values from winter to spring,. J. Geophys. Res, 113, D02312, doi:10.1029/2007JD008755, 2008.

Novakov, T., Corrigan, C.E., Penner, J.E., Chuang, C.C., Rosario, O., and Bracero, O.L.M.: Organic aerosols in the Caribbean trade winds: A natural source?, J. Geophys. Res., 102, 21307-21313, 1997.

O'Dowd, C.D., Facchini, M.C., Cavalli, F., Ceburnis, D., Mircea, M., Decesari, S., Fuzzi, S., Yoon, Y.J., and Putaud, J.-P.: Biogenically driven organic contribution to marine aerosol, Nature, 431, 676-680, 2004.

O'Dowd , C.D., Langmann, B., Varghese, S., Scannell, C., Ceburnis, D., and Facchini, M.C.: A combined organic-inorganic sea-spray source function, Geophys. Res. Lett., 35, L01801, doi:10.1029/2007GL030331, 2008.

O'Dowd, C.D., and de Leeuw, G.: Marine aerosol production: a review of the current knowledge, Phil. Trans. R. Soc. A, 365, 1753-1774, 2007.

Pfister, G.G., Emmons, L.K., Edwards, D.P., Arellano1, A., Sachse G., and Campos, T.:Variability of springtime transpacific pollution transport during 2000–2006: the INTEX-B mission in the context of previous year, Atmos. Chem. Phys., 10, 1345–1359, 2010.

Phinney, L., Leaitch, R.W., Lohmann, U., Boudries, H., Worsnop, D.R., Jayne, J.T., Toom-Sauntry, D., Wadleigh, M., Sharma, S., and Shantz, N.: Characterization of the aerosol over the sub-arctic north east Pacific Ocean, Deep-Sea Res. PT II, 53, 2410-2433, 2006.

Pincus, R., and Baker, M.B.: Effect of precipitation on the albedo susceptibility of clouds in the marine boundary layer, Nature, 372, 250– 252, 1994.

Putaud, J.-P., Van Dingenen, R., Mangoni, M., Virkkula, A., Raes, F., Maring, H., Prospero, J.M., Swietlicki, E., Berg, O.H., Hillamo, R., and Makela, T.: Chemical mass closure and assessment of origin of the submicron aerosol in the marine boundary layer and the free troposphere at Tenerife during ACE-2, Tellus, 52B, 141-168, 2000.

Quinn, P.K. and Bates, T.S.: North American, Asian, and Indian haze: Similar regional impacts on climate?, Geophys. Res. Lett., 30, 1555, doi:10.1029/2003GL016934, 2003.

Quinn, P., and Bates, T.: Regional aerosol properties: Comparisons of boundary layer measurements from ACE 1, ACE 2, Aerosols99, INDOEX, ACE Asia, TARFOX, and NEAQS, J. Geophys. Res, 110, D14202, 2005.

Quinn, P.K., Coffman, D.J., Bates, T.S., Welton, E.J., Covert, D.S., Miller, T.L., Johnson, J.E., Maria, S., Russell, L., Arimoto, R., Carrico, C.M., and Rood. M.J.: Aerosol optical properties measured on board the Ronald H. Brown during ACE-Asia as a function of aerosol chemical composition and source region, J. Geophys. Res., 109, D19S01, doi: 10.1029/2003JD004010, 2004.

Reid, J.S., Koppmann, R., Eck, T.F., and Eleuterio, D.P.: A review of biomass burning emissions part II: intensive physical properties of biomass burning particles, Atmos. Chem.. Phys., 5, 799-825, 2005.

Russell, L.M., Hawkins, L.N., Frossard, A.A., Quinn, P.K., and Bates, T.S.: Carbohydrate-like composition of submicron atmospheric particles and their production from ocean bubble bursting, PNAS, 107, 6652-6657, 2010.

Schwarz, J.P., Gao, R.S., Fahey, D.W., Thomson, D.S., Watts, L.A., Wilson, J.C., Reeves, J.M., Darbeheshti, M., Baumgardner, D.G., Kok, G.L., Chung, S.H., Schulz, M., Hendricks, J., Lauer, Al, Karcher, B., Slowik, J.G., Rosenlof, K.H., Thompson, T.L., Langford, A.O., Loewenstein, M., and Aikin, K.C.: Single-particle measurements of midlatitude black carbon andlight-scattering aerosols from the boundary layer to the lower stratosphere, J. Geophys. Res., 111, D16207, doi:10.1029/2006JD007076, 2006.

Sciare, J., Favez, O., Sarda-Estève, R., Oikonomou, K., Cachier, H., and Kazan, V.: Long-term observations of carbonaceous aerosols in the Austral Ocean atmosphere: Evidence of a biogenic marine organic source, J. Geophys. Res., 114, D15302, doi:10.1029/2009JD011998, 2009.

Schwarz, J.P., Spackman, J.R., Gao, R.S., Perring, A.E., Cross, E., Onasch, T.B., Ahern, A., Wrobel,W., Davidovits, P., Olfert, J., Dubey, M.K., Mazzoleni, C. and Fahey, D.W.: The Detection Efficiency of the Single Particle Soot Photometer, Aerosol Sci. Tech., 44, 612-628, 2010.

Sciare, J., Favez, O., Sarda-Estève, R., Oikonomou, K., Cachier, H., and Kazan, V.: Long-term observations of carbonaceous aerosols in the Austral Ocean atmosphere: Evidence of a biogenic marine organic source, J. Geophys. Res., 114, D15302, doi:10.1029/2009JD011998, 2009.

Seinfeld, J.H. and Pandis, S.N. (Eds.): Atmospheric Chemistry and Physics, 2nd ed., John Wiley & Sons, Inc., Hoboken, New Jersey, 2006.

Shaw, G., Bio-controlled thermostasis involving the sulfur cycle, Clim. Change, 5, 297-303, 1983.

Siegel, D.A., Maritorena, S., Nelson, N.B., Hansell, D.A., Lorenzi-Kayser, M.: Global distribution and dynamics of colored dissolved and detrital organic materials, J. Geophys. Res., 107, C123228, doi:10.1029/2001JC000965, 2002.

Simoneit, B. R. T., Schauer, J.J., Nolte, C.G., Oros, D.R., Elias, V.O., Fraser, M.P., Rogge, W.F., and Cass, G.R.: Levoglucosan, a tracer for cellulose in biomass burning and atmospheric particles, Atmos. Environ, 33, 173-182, 1998.

Singh, H., Anderson, B., Brune, W., Cai, C., Cohen, R., Crawford, J., Cubison, M., Czech, E., Emmons, L., Fuelberg, H., Huey, G., Jacob, D., Jimenez, J., Kaduwela, A., Kondo, Y., Mao, J., Olson, J., Sachse, G., Vay, S., Weinheimer, A., Wennberg, P., and Wisthaler, A.: Pollution influences on atmospheric composition and chemistry at high northern latitudes: Boreal and California forest fire emissions, Atmos. Environ., 44,4553 – 4564, 2010.

Spracklen, D.V., Arnold, S.R., Sciare, J., Carslaw, K.S., and Pio, C.: Globally significant oceanic source of organic carbon aerosol, Geophys. Res. Lett., 35, L12811, doi:10.1029/2008GL033359, 2008.

Staudt, A. C., Jacob, D.J., Logan, J.A., Bachiochi, D., Krishnamurti, T.N., and Sachse, G.W.: Continental sources, transoceanic transport, and interhemispheric exchange of carbon monoxide over the Pacific, J. Geophys. Res., 106, 32,571– 32,590, 2001.

Stephens, M., Turner, N., and Sandberg, J.: Particle identification by laser-induced incandescence in a solid-state laser cavity, Appl. Opt., 42(19), 3726–3736, 2003.

Sueper, D.: ToF-AMS Software Downloads, online available at: http://cires.colorado.edu/jimenez-group/ToFAMSResources/ToFSoftware/index.html, 2010.

Turekian,, V.C., Macko, S.A., and Keene, W.C.: Concentrations, isotopic compositions, and sources of size-resolved, particulate organic carbon and oxalate in near-surface marine air at Bermuda during spring, J. Geophys. Res., 108, 2003.

Turpin, B. J., Saxena, P., and Andrews, E.: Measuring and Simulating Particulate Organics in the Atmosphere: Problems and Prospects, Atmos. Environ., 34, 2983–3013, 2000.

Twomey, S.: The influence of pollution on the short wave albedo of clouds, J. Atmos. Sci., 34, 1149–1152, 1977.

Vignati, E., Facchini, M.C., Rinaldi, M., Scannell, C., Ceburnis, D., Sciare, J., Kanakidou, M., Myriokefalitakis, S., Dentener, F., O'Dowd, C.D.: Global scale emission and distribution of sea-spray aerosol: Sea-salt and organic enrichment, Atmos. Environ., 44, 670-677, 2010.

Virkkula, A., Ahlquist, N. C., Covert, D. S., Arnott, W. P., Sheridan, P. J., Quinn, P. K. and Coffman, D. J.: Modification, Calibration and a Field Test of an Instrument for Measuring Light Absorption by Particles, Aerosol Sci. Technol., 39, 68, 2005.

Volkamer, R., Coburn, S., Dix, B., and Sinreich, R.: The Eastern Pacific Ocean is a source for short lived trace gases: Glyoxal and Iodine Oxide, Clivar Exchanges, 15(2), 30–33, 2010.

Weber, J., McMurry, P.H., Mauldin, L., Tanner, D.J., Eisele, F.L., Brechtel, F.J., Kreidenweis, S.M., Kok, G.L., Schillawski, R.D., and Baumgardner, D.: A study of new particle formation and growth involving biogenic and trace gas species measured during ACE1, J. Geophys. Res., 103, 16385–16396, 1998.

Weingartner, E., Saathoff, H., Schnaiter, M., Streit, N., Bitnar, B. and Baltensperger, U.: Absorption of Light by Soot Particles: Determination of the Absorption Coefficient by Means of Aethelometers, Aerosol Science , 34: 1445–1463, 2003.

Westervilt, D.M., Moore, R.H., Nenes, A., Adams, P.J.: Effect of primary organic sea spray emissions on cloud condensation nuclei concentrations, Atmos. Chem. Phys. Discuss., 11, 5757-5784, doi:10.5194/acpd-11-5757-2011, 2011.

Wood, R., Bretherton, C.S., Leon, D., Clarke, A.D., Zuidema, P., Allen, G., and Coe, H.: An aircraft case study of the spatial transition from closed to open mesoscale cellular convection, Atmos. Chem. Phys., 11, 2341-2370, doi:10.5194/acp-11-2341-2011, 2011a.

Wood, R., Bretherton, C.S., Mechoso, C.R., Weller, R.A., Huebert, B., Straneo, F., Albrecht, B.A., Coe, H., Allen, G., Vaughan, G., Daum, P., Fairall, C., Chand, D., Gallardo, K., Garreaud, R., Grados Quispe, C., Covert, D.S., Bates, T.S., Krejci, R., Russell, L.M., de Szoeke, S., Brewer, A., Yuter, S.E., Springston, S.R., Chaigneau, A., Toniazzo, T., Minnis, P., Palikonda, R., Abel, S.J., Brown, W.O.J., Williams, S., Fochesatto, J., and Brioude, J.: The VAMOS Ocean-Cloud-Atmosphere-Land Study Regional Experiment (VOCALS-Rex): goals, platforms, and field operations, Atmos. Chem. Phys., 11, 627-654, doi:10.5194/acp-11-627-2011, 2011b.

Yoon, Y. J., Ceburnis, D., Cavalli, F., Jourdan, O., Putaud, J.-P., Facchini, M.C., Decesari, S., Fuzzi, S., Sellegri, K., Jennings, S.G., and O'Dowd, C.D.: Seasonal characteristics of the physiochemical properties of North Atlantic marine atmospheric aerosols, J. Geophys. Res.,112, D04206, doi:10.1029/2005JD007044, 2007.

Zhang, X., Smith, K.A., Worsnop, D.R., Jimenez, J.L., Jayne, J.T., and Kolb, C.E.: A numerical characterization of particle beam collimation by an aerodynamic lens-nozzle system: Part I. An individual lens or nozzle, Aerosol Sci. Technol., 36, 617-631, 2002.

Zhang, X.F., Smith, K.A., Worsnop, D.R., Jimenez, J., Jayne, J.T., Kolb, C.E., Morris, J., and Davidovits, P.: A numerical characterization of particle beam collimation by an aerodynamic lens-nozzle system: Part II. Integrated aerodynamic lens-nozzle system, Aerosol Sci. Technol., 38, 619-638, 2004.

Zhou, J., Hygroscopic properties of atmospheric aerosol particles in various environments, Ph.D. thesis, 166 pp., ISBN 91-7874-120-3, LUTFD2/(TFKF-1025)/1-166/(2001), Lund University, Lund, Sweden, 2001.

Zorn, S.R., Drewnick, F., Schott, M., Hoffmann, T., and Borrmann, S.: Characterization of the South Atlantic marine boundary layer aerosol using an aerodyne aerosol mass spectrometer, Atmos. Chem. Phys., 8, 4711-4728, 2008.